

## Article

# Towards a Complete Exploitation of Brewers' Spent Grain from a Circular Economy Perspective

Chiara Allegretti <sup>1</sup>, Emanuela Bellineto <sup>1</sup>, Paola D'Arrigo <sup>1,2,\*</sup>, Gianmarco Griffini <sup>1</sup>, Stefano Marzorati <sup>2</sup>,  
Letizia Anna Maria Rossato <sup>1</sup>, Eleonora Ruffini <sup>1</sup>, Luca Schiavi <sup>3</sup>, Stefano Serra <sup>2,\*</sup>, Alberto Strini <sup>3</sup>,  
Davide Tessaro <sup>1</sup> and Stefano Turri <sup>1</sup>

- <sup>1</sup> Department of Chemistry, Materials and Chemical Engineering "Giulio Natta", Politecnico di Milano, p.zza L. da Vinci 32, 20133 Milano, Italy; chiara.allegretti@polimi.it (C.A.); emanuela.bellineto@polimi.it (E.B.); gianmarco.griffini@polimi.it (G.G.); letiziaanna.rossato@polimi.it (L.A.M.R.); eleonora.ruffini@mail.polimi.it (E.R.); davide.tessaro@polimi.it (D.T.); stefano.turri@polimi.it (S.T.)
- <sup>2</sup> Istituto di Scienze e Tecnologie Chimiche "Giulio Natta", Consiglio Nazionale delle Ricerche (SCITEC-CNR), via Luigi Mancinelli 7, 20131 Milano, Italy; stefano.marzorati@scitec.cnr.it
- <sup>3</sup> Istituto per le Tecnologie della Costruzione, Consiglio Nazionale delle Ricerche (ITC-CNR), via Lombardia 49, 20098 San Giuliano Milanese, Italy; luca.schiavi@itc.cnr.it (L.S.); alberto.strini@itc.cnr.it (A.S.)
- \* Correspondence: paola.darrigo@polimi.it (P.D.); stefano.serra@cnr.it (S.S.); Tel.: +39-2-23993075 (P.D.); +39-2-23993076 (S.S.)

**Abstract:** In the present work, brewers' spent grain (BSG), which represents the major by-product of the brewing industry, was recovered from a regional brewery and fractionated in order to obtain a complete valorization. In particular, the whole process was divided in two main parts. A first pretreatment with hot water in an autoclave allowed the separation of a solution containing the soluble proteins and sugars, which accounted for 25% of the total starting biomass. This first step allowed the preparation of a medium that was successfully employed as a valuable growing medium for different microbial fermentations, leading to valuable fungal biomass as well as triglycerides with a high content of linear or branched fatty acids, depending on the microorganism used. The solid water-insoluble residue was then submitted to a lignocellulose deep eutectic solvent-mediated fractionation, which allowed the recovery of two important main fractions: BSG cellulose and BSG lignin. The latter product was tested as potential precursor for the development of cement water reducers with encouraging results. This combination of treatments of the waste biomass appeared to be a promising sustainable strategy for the development of the full exploitation of BSG from a circular economy perspective.

**Keywords:** brewers' spent grain; deep eutectic solvents; fermentation; *Phaffia rhodozyma*; branched chain fatty acids; lignin; cement plasticizers; circular economy



**Citation:** Allegretti, C.; Bellineto, E.; D'Arrigo, P.; Griffini, G.; Marzorati, S.; Rossato, L.A.M.; Ruffini, E.; Schiavi, L.; Serra, S.; Strini, A.; et al. Towards a Complete Exploitation of Brewers' Spent Grain from a Circular Economy Perspective. *Fermentation* **2022**, *8*, 151. <https://doi.org/10.3390/fermentation8040151>

Academic Editor:  
Mohammad Taherzadeh

Received: 10 March 2022  
Accepted: 26 March 2022  
Published: 29 March 2022

**Publisher's Note:** MDPI stays neutral with regard to jurisdictional claims in published maps and institutional affiliations.



**Copyright:** © 2022 by the authors. Licensee MDPI, Basel, Switzerland. This article is an open access article distributed under the terms and conditions of the Creative Commons Attribution (CC BY) license (<https://creativecommons.org/licenses/by/4.0/>).

## 1. Introduction

The European Commission has recently presented, under the Green Deal strategy and from the view of a change of paradigm of the industrial production, the so-called Circular Economy Action Plan [1]. This pivotal document includes proposals for sustainable product design, consumer and public purchaser empowerment, and circularity in production processes. The latter concept includes the creation of a well-functioning market for secondary raw materials: low-value by-products of traditional production chains, usually disposed of as waste, that can be fed back into the economy as new raw materials. This serves the dual purpose of decreasing waste production, with its many environmental problems, and finding alternatives for supplying production chains.

From this perspective, increasing attention has been paid to brewers' spent grain (BSG), as documented by the explosion of references in the recent literature (see Figure 1).

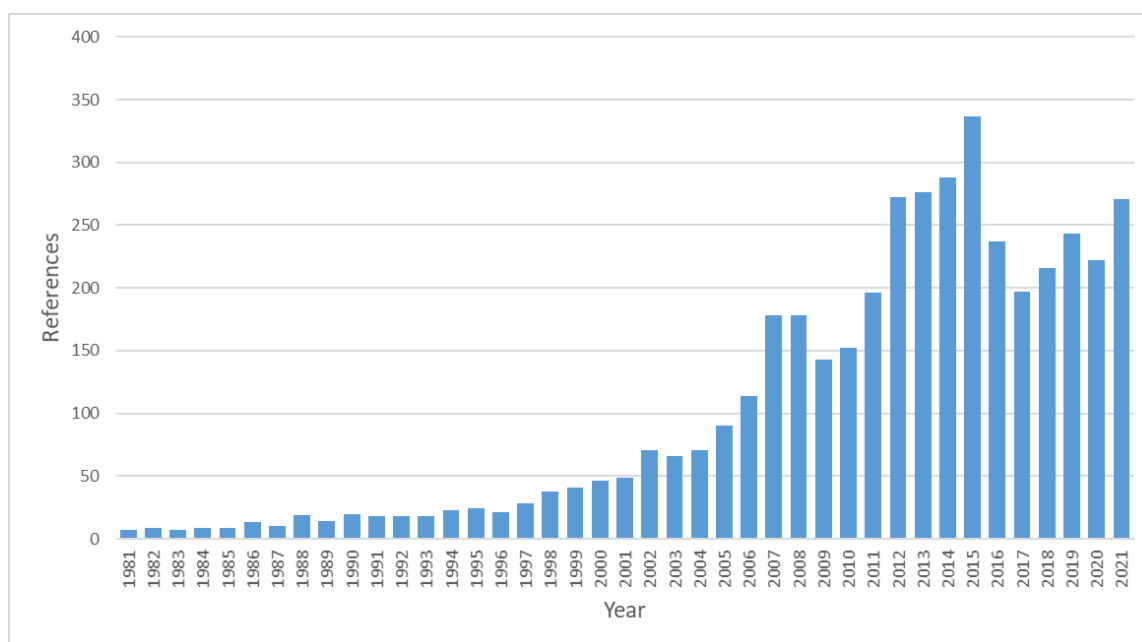


**Figure 1.** Number of references relative to brewers' spent grain as retrieved by Sci-Finder<sup>n</sup> (CAS, American Chemical Society) on 8 March 2022.

Spent grain constitutes by far the major by-product of the brewing industry, constituting about 85% of the total by-products generated in the process. It was calculated that the production of 100 L of beer results in the generation of around 20 kg of BSG, or 14 kg if we consider the dry weight [2]. According to Eurostat, 30–40 billion litres of beer are produced in Europe every year, translating into the production of 6–8 million tons of BSG. This huge amount of by-products, however, has to be quickly disposed of, since the high amount of humidity, around 75%, promotes the growth of spoilage microorganisms and its simple presence attracts rodents in the brewery. Most frequently, BSG is immediately delivered to neighboring farms, where it is employed for feeding cattle or as a fertilizer in agriculture [3,4]. Of course, problems arise when breweries are located in heavily urbanized areas or in remote non-agricultural areas (for example, in the mountains): in these cases BSG cannot be rapidly delivered and has to be disposed of, constituting a waste of resource and a significant cost for the brewery. The valorization of BSG from a circular economy perspective would thus contribute not only to saving resources, reducing land use, and decreasing the carbon footprint of the brewing process, but would also help the establishment of novel waste processing streams, thus introducing little but significant societal changes. A necessary condition to promote recovery and treatment of BSG is the obtainment of high added-value products which would justify a general interest that would cover the processing costs.

Since BSG is a complex matrix composed of approximately 15–25% proteins, 50–70% fiber (hemicellulose, cellulose, and lignin), 5–10% fats, and 2–5% ashes [2,5–8], a careful fractionation is necessary to obtain homogeneous precursors of the target compounds, ensuring the maximum exploitation of the whole material. In this context, a number of studies have described the use of BSG as a source of specific precursors to be employed for the preparation of products of commercial relevance such as alimentary proteins and fiber [9], enzymes, biopolymers [10], saccharides, and lignin [11].

Despite the growing industrial and scientific interest in BSG disposal, very few researchers have investigated the complete valorization of this waste material [12,13]. According to the concept of the circular economy, an industrial process exploiting BSG should rely on the exploitation of all its chemical components with the production of different products of commercial interest. The aim of such a conceived process is the complete recycling of

the starting waste material with the concomitant production of added-value compounds, so as to warrant the economic sustainability of the whole cycle.

Following this approach, an innovative process for complete BSG exploitation has been here investigated. Accordingly, a scalable procedure for the separation of the above-mentioned material in three different fractions is summarized in Figure 2.

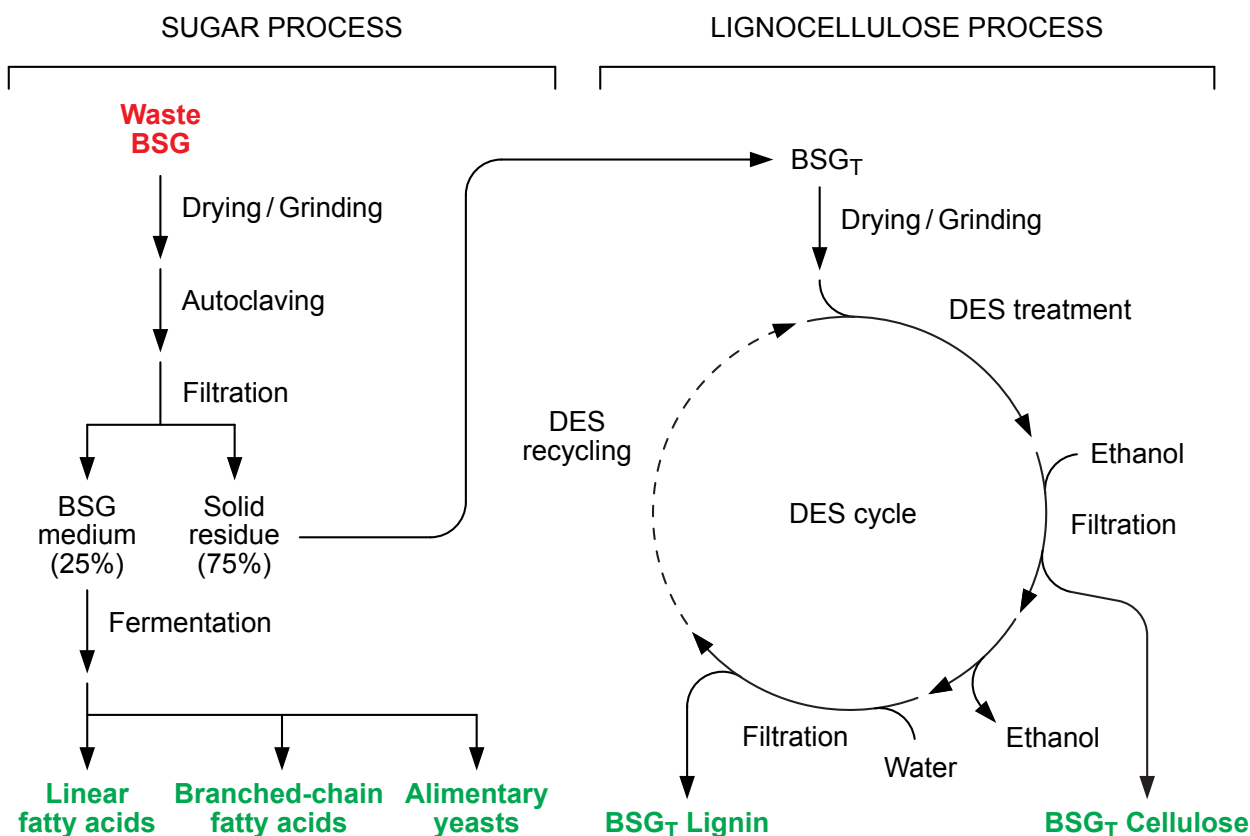


**Figure 2.** Integrated process for complete BSG waste valorization, subdivided into a sugar process and a lignocellulose process. In the first one, BSG waste is autoclaved and then separated into a sugar-rich medium and a solid residue. Different bioderivatives can be obtained from the former by fermentation. The solid lignocellulosic residue (BSG<sub>T</sub>) is instead fractionated with DES to obtain purified lignin and cellulose. The DES is then recovered and recycled in a closed-loop process.

Starting from wet BSG waste recovered from a local brewery, the process has been divided into two main parts consisting of the sequential application of different chemical-physical treatments. A first BSG extraction using water at high temperature allowed the separation of the soluble proteins and polysaccharides (about 25% of the starting BSG) that constitute the basis for a fermentation substrate (BSG medium) and are subsequently transformed into bioderivatives (the sugar process). The solid residue of the first extraction undergoes instead a fractionation by means of a deep eutectic solvent-mediated process leading to the biomass separation in two defined components, namely BSG<sub>T</sub> Lignin and BSG<sub>T</sub> Cellulose (the lignocellulose process). Therefore, the integrated process leads to the separation of the three main components of BSG (fermentable soluble fraction, cellulose, and lignin). Of the latter, the soluble fraction and lignin were specifically analyzed in this work.

In particular the first fraction was used as a specific medium for microbial fermentation and BSG<sub>T</sub> Lignin was investigated as a potential renewable source for the development of enhanced water reducer for concrete production. The BSG extract turned out to be very rich in soluble starch and contained only a minor amount of other nutrients such as proteins and oligosaccharides. Therefore, in order to ensure a nitrogen content suitable for microbial growth, ammonium sulphate was added to the aqueous extract.

The obtained BSG medium can furnish the proper nutrients for different microbial strains; more specifically, fungal and bacterial strains that are able to grow on polysaccharides or have been already employed in the transformation of polysaccharide-containing waste materials were here selected [14,15]. Among the plethora of described microorganisms, the basidiomycetous yeast *Phaffia rhodozyma*, the oleaginous yeast *Yarrowia lipolytica* and selected bacterial strains from the genus *Rhodococcus* and *Streptomyces* were singled out. The results of the present study pointed to the potential employment of the obtained microbial biomass in aquaculture, human alimentation, and biodiesel production.

In the second part of the process (the so-called lignocellulose process, as indicated in Figure 2), the treated BSG (BSG<sub>T</sub>) underwent a deep eutectic solvent (DES)-based treatment aiming to deconstruct the lignocellulosic skeleton in order to obtain the separation of the two main components of the biomass, cellulose and lignin. Lignin is the most abundant aromatic biopolymer in nature, and despite its chemical recalcitrance, its possible exploitation is widely studied for several application fields [16–18], including materials science [19–22], materials engineering [23,24], agriculture [25], and energy [26–28]. An industrially attractive lignin application is the formulation of cement water reducers, an important component for the production of concrete [29]. In recent years, a renewed interest for lignin in this specific field was spurred by several research efforts aimed at the development of renewable, high-performance lignin-based concrete water reducers capable of competing with modern synthetic products [30–32]. This was carried out by using non-sulfonated lignins as a starting point, such as those deriving either from the soda process [33] or from formic acid extraction [34]. Any sustainable process delivering lignin as a by-product is thus a potential resource for the development of renewable cement water reducers in a circular economy approach. In the present study, a first evaluation of the suitability of the BSG<sub>T</sub> Lignin for this specific application was carried out implementing a laboratory rheological test on cement pastes that demonstrated a water reduction performance equivalent to those of Protobind 1000, a well-known commercial soda lignin.

## 2. Materials and Methods

### 2.1. Materials and General Methods

All air- and moisture-sensitive reactions were carried out using dry solvents and under a static atmosphere of nitrogen. Choline chloride (C0329), betaine glycine (B0455) and L-lactic acid (L0165) were provided by TCI (Milano, Italy). BSG was provided by the Brewery “L’Orso Verde” (Busto Arsizio, Italy). Protobind 1000, a mixed wheat straw/sarkanda grass lignin from soda pulping of non-woody biomass) was provided by Tanovis (Alpnach, Switzerland). Riboflavin was purchased from Health Leads UK Ltd., (Horeb, UK). The other reagents and the employed solvents were purchased from Merck (Merck Life Science S.R.L., Milan, Italy) and used without further purification.

Reference standard samples of C<sub>12</sub>–C<sub>19</sub> branched-chain fatty acids (BCFAs) were prepared as described in a work in preparation.

### 2.2. Microorganisms and Growth Media

*Yarrowia lipolytica* (DSM 8218), *Yarrowia lipolytica* (DSM 70562), *Phaffia rhodozyma* = *Xanthophyllomyces dendrorhous* (DSM 5626), and *Rhodococcus opacus* (DSM 43205) were purchased from DSMZ GmbH collection (Braunschweig, Germany).

*Streptomyces cavourensis* subsp. *cavourensis* (DSM 112466) and *Streptomyces albidoflavus* (DSM 112467) were isolated as axenic cultures in our laboratory, then identified through the 16S rRNA gene sequencing and finally deposited in the DSMZ GmbH collection (Braunschweig, Germany) under the collection number given in brackets.

The growth media used in this work were YUM (Yeasts Universal Medium) implemented with 20 mg/L of riboflavin, TSB (tryptic soy broth), GYM medium, and BSG medium.

YUM medium composition: yeast extract (3 g/L), malt extract (3 g/L), peptone from soybeans (5 g/L), glucose (10 g/L).

TSB medium composition: casein peptone (17 g/L), glucose (2.5 g/L), soya peptone (3 g/L), NaCl (5 g/L),  $K_2HPO_4$  (2.5 g/L).

GYM medium composition: glucose (4 g/L), yeast extract (4 g/L), malt extract (10 g/L).

BSG medium: BSG aqueous extract,  $(NH_4)_2SO_4$  (3 g/L), yeast extract (1 g/L), and trace elements solution (10 mL/L). For bacteria fermentation, a further 1 g/L of NaCl was added. The preparation of the BSG aqueous extract is described in the context of the BSG treatment procedure (Section 2.3).

YUM was used for the pre-growth of *Yarrowia lipolytica* and *Xanthophyllomyces dendrorhous*, TSB was used for the pre-growth of *Rhodococcus opacus*, and GYM was used for the pre-growth of *Streptomyces cavourensis* subsp. *cavourensis* and *Streptomyces albidoflavus*.

Trace elements solution:  $FeCl_3$  (50 mM),  $CaCl_2$  (20 mM),  $MnCl_2$  (10 mM),  $ZnSO_4$  (10 mM),  $CoCl_2$  (2 mM),  $CuCl_2$  (2 mM),  $NiCl_2$  (2 mM),  $Na_2MoO_4$  (2 mM),  $Na_2SeO_3$  (2 mM),  $H_3BO_3$  (2 mM).

### 2.3. BSG Aqueous Extraction

BSG waste was obtained as wet residue directly from the brewery within 12 h after a batch of beer production. This material was brought to dryness in a ventilated oven (60 °C, 24 h) and was finely ground with the help of an electric mixer. The obtained BSG, designated as BSG<sub>U</sub> (untreated BSG) contained 4.3% residual humidity and was stored sealed and refrigerated (4 °C).

BSG<sub>U</sub> (40 g) was suspended in deionized water (700 mL) and was heated in an autoclave (121 °C, 15 min). The solid was filtrated, washed three times with deionized water (3 × 250 mL) and was dried in a ventilated oven (60 °C, 24 h) leading to 29.8 g of treated BSG, named BSG<sub>T</sub>, (4.1% of residual humidity). BSG<sub>T</sub> was then processed further to separate cellulose and lignin (see Section 2.5) whereas the combined liquid phases were used for the preparation of the BSG microbial growth medium. Accordingly, ammonium sulfate (4.5 g), yeast extract (1.5 g), and trace elements solution (15 mL) were added to the extract. Hence, the final volume of the liquid was adjusted to 1.5 L by addition of further deionized water and the obtained medium was sterilized by autoclaving (121 °C, 15 min).

### 2.4. Evaluation of Fermentation with BSG Microbial Growth Medium

The BSG medium prepared as described above was used for the growth of five different strains, namely *Yarrowia lipolytica* (DSM 8218), *Yarrowia lipolytica* (DSM 70562), *Xanthophyllomyces dendrorhous* (DSM 5626), *Rhodococcus opacus* (DSM 43205), *Streptomyces cavourensis* subsp. *cavourensis* (DSM 112466), and *Streptomyces albidoflavus* (DSM 112467). The experiments were carried out in triplicate and the presented results are the media of three experimental data.

Each fermentation trial was performed using a 5 L bioreactor (Biostat A BB-8822000, Sartorius-Stedim (Göttingen, Germany) loaded with 1.5 L of BSG medium. Stirring and aeration were set at 200 rpm and 0.6 L/L/min, respectively whereas the temperature, the pH, and the fermentation duration were set depending on the strain used (Table 1). As soon as the fermentation was stopped, the biomass was collected by centrifugation and was freeze-dried in high vacuum (0.05 mmHg) until the sample reached constant weight. The obtained dry biomass was treated, under a static atmosphere of nitrogen, with aqueous NaOH (10% w/v, 16 mL per gram of biomass) and methanol (4 mL per gram of biomass). The mixture was vigorously stirred and was heated at reflux for 6 h. Hence, the reaction was cooled (0 °C), was acidified by dropwise addition of concentrated HCl aqueous (37% w/v), and was extracted twice with ethyl acetate. The combined organic phases were washed in turn with water and with brine, then were dried ( $Na_2SO_4$ ), and were concentrated under reduced pressure. The residue consisted of a mixture of free fatty acids. The presence of other metabolites was negligible, as indicated by the chromatographic

purification affording the fatty acids mixture with a weight loss of only 10%. A sample of this mixture was treated at 0 °C with an excess of an ethereal solution of freshly-prepared diazomethane. The obtained methyl esters mixture was submitted to GC–MS analysis.

**Table 1.** Production of biomass and fatty acids using the BSG medium and some selected microbial strains.

Entry	Microbial Strain	Growth Conditions <sup>1</sup>	Biomass Productivity <sup>2</sup>	Fatty Acid Productivity <sup>3</sup>
1	<i>Phaffia rhodozyma</i> (DMS 5626)	6 days at 22 °C, pH 6.5	3.6 g/L (135 g/Kg BSG)	-
2	<i>Yarrowia lipolytica</i> (DSM 8218)	4 days at 25 °C, pH 6.5	1.5 g/L (55 g/Kg BSG)	200 mg/L (7.5 g/Kg BSG)
3	<i>Yarrowia lipolytica</i> (DSM 70562)	4 days at 25 °C, pH 6.5	1.6 g/L (61 g/Kg BSG)	220 mg/L (8.2 g/Kg BSG)
4	<i>Rhodococcus opacus</i> (DSM 43205)	4 days at 28 °C, pH 7.0	2.4 g/L (89 g/Kg BSG)	547 mg/L (20.5 g/Kg BSG)
5	<i>Streptomyces cavourensis</i> (DSM 112466)	4 days at 28 °C, pH 7.0	2.1 g/L (80 g/Kg BSG)	220 mg/L (8.2 g/Kg BSG)
6	<i>Streptomyces albidoflavus</i> (DSM 112467)	4 days at 28 °C, pH 7.0	1.7 g/L (64 g/Kg BSG)	180 mg/L (6.7 g/Kg BSG)

<sup>1</sup> Each microbial growth was performed in a 5 L bioreactor, using 1.5 L of BSG medium. Stirring and aeration were set at 200 rpm and 0.6 L/L/min, respectively. <sup>2</sup> The biomass was collected by centrifugation as soon as the fermentation was stopped and then was freeze-dried. The biomass productivity is indicated as both grams of dried biomass produced starting from one liter of BSG medium and grams of dried biomass produced starting from one kilogram of dried BSG<sub>U</sub> (value in brackets). <sup>3</sup> The fatty acid productivity is indicated as both milligrams of the fatty acid mixture produced starting from one liter of BSG medium and grams of the fatty acid mixture produced starting from one kilogram of dried BSG<sub>U</sub> (value in brackets).

### 2.5. Preparation of DESs

The DESs were prepared by mixing anhydrous hydrogen bond acceptor (HBA) with hydrogen bond donor (HBD) in the determined molar ratio (see Section 3.2.1) and stirred in a closed flask, at 120 °C for 4 h until the liquid phase appeared completely homogeneous and clear. The product was then dried under vacuum and stored at room temperature in a dessicator in the presence of anhydrous calcium chloride until further use. The <sup>1</sup>H NMR spectrum of the selected DES (choline chloride/L-lactic acid 1/5) for the full fractionation is reported in Supplementary Materials Figure S1. The recycling of this DES has been performed for three cycles without any modifications as confirmed by <sup>1</sup>H NMR spectrum reported in Supplementary Materials Figure S2.

### 2.6. BSG Treatment with DES

BSG<sub>U</sub> (25 g) was suspended in DES choline chloride/L-lactic acid 1/5 (250 mL) at 130 °C in a round-bottom flask under magnetic stirring for 24 h. After cooling, ethanol (500 mL) was then added gradually over 2 h in order to precipitate the cellulose fraction. The pellet was separated by centrifugation and filtration, washed many times with ethanol and dried to give a final solid BSG<sub>U</sub> Cellulose (4–6 g) with a yield of 17–25% (*w/w* initial biomass). The filtrate was then concentrated by rotary evaporation under vacuum to eliminate ethanol. Water (500 mL) was then added and the suspension was stirred for 24 h at 4 °C. The obtained precipitate was then centrifuged, filtered, and washed three times for 1 h with a solution of water/ethanol 9/1. After centrifugation, filtration, and solvent evaporation, the final fraction (BSG<sub>U</sub> Lignin, 2.4 g) was recovered with a final yield of 10% (*w/w* initial biomass).

Thirty grams of BSG<sub>T</sub>, obtained as the effluent of the sugar process performed on 40 g of starting BSG was then treated with 150 mL of DES in the same conditions and procedure as described just above. The final products were: the BSG<sub>T</sub> Cellulose fraction (12 g, 40%

yield, global yield 30% (*w/w* initial biomass), and the lignin fraction BSG<sub>T</sub> Lignin (4 g, 13.3% yield, global yield 10% (*w/w* initial biomass)).

### 2.7. Lignin Solubility in Organic Solvents

Lignin solubility in the different solvents was determined by treating 1 g of the analyzed lignin with 10 mL of the solvent under stirring at 400 rpm. Each test was carried out overnight at room temperature. The suspension was then filtered and the solvent was evaporated at reduced pressure, and the final residue was dried until a constant weight was achieved prior to quantification.

### 2.8. Instruments and Analytic Condition

#### 2.8.1. Thin Layer Chromatography

Thin layer chromatography (TLC) Merck silica gel 60 F<sub>254</sub> plates (Merck Millipore, Milan, Italy) were used for analytical TLC. Preparative column chromatography was performed with silica gel.

#### 2.8.2. <sup>1</sup>H NMR

<sup>1</sup>H NMR spectra were obtained using a Bruker-AC-400 spectrometer (Billerica, MA, USA) at 400 MHz and 348 K; the samples were externally locked using D<sub>2</sub>O in a coaxial insert tube and the chemical shifts were recorded in ppm.

#### 2.8.3. Gas-Chromatography/Mass Spectrometry

The gas-chromatography–mass spectrometry (GC–MS) apparatus was a HP-6890 gas chromatograph equipped with a 5973 mass detector and a HP-5MS column (30 m × 0.25 mm, 0.25 μm film thickness; Hewlett Packard, Palo Alto, CA, USA). The separation of the fatty acid methyl esters was performed with the following temperature program: 120 °C (3 min)—12 °C/min—195 °C (10 min)—12 °C/min—300 °C (10 min); carrier gas: He; constant flow 1 mL/min; split ratio: 1/30.

#### 2.8.4. Gel Permeation Chromatography

A Waters 510 HPLC system equipped with a refractive index detector was used for gel permeation chromatography (GPC) analyses. Tetrahydrofuran (THF) was used as eluent. The analyzed lignin sample (volume 200 μL, concentration 1 mg/mL in THF) was injected into a system of three columns connected in series (Ultrastrygel models HR2, HR3 and HR4, dimensions 7.8 mm (inner diameter) × 300 mm (length), provided by Waters) packed with 5 μm spherical particles and covering a broad range of molecular weights (10<sup>2</sup>–10<sup>5</sup> g/mol). The analysis was performed at 30 °C at a flow rate of 0.5 mL/min. The GPC system was calibrated against polystyrene standards in the 10<sup>2</sup>–10<sup>4</sup> g/mol molecular weight range. To allow complete solubility in the THF eluent, before the analysis, the parent lignin and the fractions were acetylated following a standard literature procedure [35]. Briefly the estimation of the number-average and weight-average molecular weights ( $M_n$  and  $M_w$  respectively) of the obtained lignin fractions was performed excluding the signals related to the solvent (THF) and the solvent stabilizer (butylated hydroxytoluene), visible at long elution times (>29.5 min).

#### 2.8.5. Total Sugars Quantification

Two stock solutions were prepared fresh every time with a protocol previously described with some modifications [36]. Solution A was prepared by dissolution of 19 mg of disodium 2,2-bicinchoninate, 0.543 g of Na<sub>2</sub>CO<sub>3</sub> and 0.242 g of NaHCO<sub>3</sub> in 10 mL of distilled water. Solution B was obtained by dissolution of 12.4 mg of CuSO<sub>4</sub>·5H<sub>2</sub>O and 12.6 mg of L-serine in 10 mL of distilled water. BCA working solution was freshly prepared just before use by mixing equal volumes of solution A and solution B.

*Method 1:* This method was performed for aqueous soluble samples. In detail: 1 mL of BCA working solution was added to 1 mL of sample in a vial and incubated at 70 °C

for 30 min. The vials were cooled at room temperature, 1 mL of mixture was transferred to a cuvette, and the absorbance was determined at 560 nm. The total reducing sugar value in the samples was then read from the glucose calibration curve a (see Supplementary Materials Figure S3). The calibration curve was established by using a glucose solution as standard in the 0–72  $\mu\text{M}$  concentration range.

*Method 2:* This method was performed for aqueous-insoluble samples that showed dimethylsulfoxide (DMSO) solubility. The samples were prepared by dissolving lignin in DMSO with a final concentration of 2 mg/mL. For each determination, 5  $\mu\text{L}$  of the solution were then mixed with 995  $\mu\text{L}$  of water and 1 mL of BCA working solution in a vial and incubated at 70 °C for 30 min. The vials were cooled at room temperature, 1 mL of mixture was transferred to a cuvette, and the absorbance was determined at 560 nm. In all cases, the contribution of DMSO to color development was measured and subtracted from the final value. The calibration curve b (see Supplementary Materials Figure S4) was established by using a glucose solution as standard in the 0–280  $\mu\text{M}$  concentration range.

*Method 3:* In order to determine the abundance of polysaccharides in lignin samples, acid hydrolysis of the samples was performed by incubation of 100 mg of sample with 100 mL water/HCl 37% 6/4 for 2.5 h at 80 °C. The mixture was then set to neutral pH and then filtered. The total reducing sugar concentration in the filtrate was then measured with method 2.

#### 2.8.6. Phenolic Hydroxyl Group Determination

The total phenolic content of lignins was determined by a modified Folin–Ciocalteu (FC) protocol with some modifications to the sample preparation step previously described [37]. The samples were dissolved in DMSO with a final concentration of 2 mg/mL. DMSO was chosen because, being completely miscible in water, it allowed complete lignin solubilization and did not interfere with the FC assay. For each determination, 5  $\mu\text{L}$  of the working solution (or the standard solution) were then mixed with 120  $\mu\text{L}$  of deionized water, 125  $\mu\text{L}$  of FC reagent (Sigma 47641), and kept for 6 min at room temperature after 30 s of vortex stirring. Then, after the addition of 1.25 mL of 5% sodium carbonate and mixing, the vial was incubated in a thermoshaker at 40 °C for 30 min. The reaction mixture absorbance was measured using a UV–Vis spectrophotometer (Jasco V-560) equipped with a temperature-controlled cuvette holder and a thermostatic water bath (Haake K10, Karlsruhe, Germany). All spectrophotometric measurements were carried out at 760 nm, 25 °C, using a 1 cm optical path cuvette and deionized water as blank sample. Vanillin was chosen as the reference standard. The calibration curve was constructed with nine different vanillin solutions in DMSO with concentration in the range 0–500  $\mu\text{g}/\text{mL}$  (see Supplementary Materials Figure S5). Each FC assay determination was carried out in triplicate.

#### 2.8.7. $^{31}\text{P}$ NMR Analysis

$^{31}\text{P}$  NMR spectroscopic analyses were recorded on a Bruker Instrument AVANCE400 spectrometer (Milano, Italy). Acquisition and data treatment were performed with Bruker TopSpin 3.2 software (Milano, Italy). The spectra were collected at 29 °C with a 4 s acquisition time, 5 s relaxation delay, and 256 scans. Prior to analysis, samples were dried for 24 h under vacuum and then derivatized according to the following procedure.

The sample (40 mg) was completely dissolved in 300  $\mu\text{L}$  of *N,N*-dimethylformamide. To this solution, the following components were added: 200  $\mu\text{L}$  of dry pyridine, 100  $\mu\text{L}$  of solution of internal standard (10 mg of Endo-*N*-hydroxy-5-norbornene-2,3-dicarboximide (Sigma 226378) dissolved in 0.5 mL of a mixture of pyridine and  $\text{CDCl}_3$  1.6:1 *v/v*), 50  $\mu\text{L}$  of a relaxation agent solution (5.7 mg of chromium (III) acetylacetonate (Sigma 574082) dissolved in 0.5 mL of a mixture of pyridine and  $\text{CDCl}_3$  1.6:1 *v/v*), 100  $\mu\text{L}$  of 2-chloro-4,4,5,5-tetramethyl-1,3,2-dioxaphospholane (Sigma 447536), and at the end 200  $\mu\text{L}$   $\text{CDCl}_3$ . The solution was centrifuged and/or filtered if necessary. All chemical shifts reported

were related to the reaction product of the phosphorylating agent with water, which gave a signal at 132.2 ppm.

#### 2.8.8. Fourier-Transform Infrared Spectroscopy

Fourier-transform infrared spectroscopy (FTIR) was performed by a Nicolet Netxus 760 FTIR spectrophotometer. The samples were prepared by pressing the biomass powders with KBr powder to obtain thin discs. Spectra were obtained in transmission mode, at room temperature, in air, by recording 64 accumulated scans at a resolution of  $4\text{ cm}^{-1}$  in the  $4000\text{--}500\text{ cm}^{-1}$  wavenumber range.

#### 2.8.9. Differential Scanning Calorimetry

Differential scanning calorimetry (DSC) was employed to investigate the thermal transitions of lignin samples. Measurements were carried out on 10–15 mg samples by means of a Mettler-Toledo DSC 823e instrument. Three runs (heating/cooling/heating) were performed: from  $25\text{ }^{\circ}\text{C}$  to  $150\text{ }^{\circ}\text{C}$  to remove water from samples, from  $150\text{ }^{\circ}\text{C}$  to  $25\text{ }^{\circ}\text{C}$ , and from  $25\text{ }^{\circ}\text{C}$  to  $200\text{ }^{\circ}\text{C}$ , at a scan rate of  $20\text{ }^{\circ}\text{C}/\text{min}$  under nitrogen flux. The glass transition temperature ( $T_g$ ) of the samples was evaluated as the inflection point in the second heating run.

#### 2.9. Water Reduction in Cement Pastes

A preliminary estimation of the water reduction capability of recovered lignins was carried out evaluating the relative Bingham dynamic yield torque of cement pastes containing 0.2% of lignin ( $w/w$  relative to dry cement) at different water/cement ( $w/c$ ) ratio [38]. This allowed us to compare the water reduction attainable from each lignin in order to obtain a cement paste with the same yield torque of a pure cement paste with 0.45  $w/c$  ratio, taken as reference. The water reduction was evaluated for BSG<sub>U</sub> Lignin, for BSG<sub>T</sub> Lignin and for the commercial soda lignin Protobind 1000. For each rheological measurement an alkaline (NaOH) lignin solution (10%  $w/w$  lignin/water) was prepared taking care to obtain a final content of 0.4 g of lignin and 3.6 g of water. A cement paste was prepared mixing 200 g of ordinary Portland cement (CEM I 42.5 R according to EN 197-1 standard) with water in the required amount minus 3.6 g that was added later to the lignin solution. The cement/water paste was then stirred manually for 2 minutes, after which the lignin solution was added. The paste was further stirred for 2 min and finally transferred into the rheometer cup.

A rotational rheometer (RheolabQC, Anton Paar GmbH, Graz, Austria) provided with a 30 mm diameter four blade stirrer and a 42 mm diameter sandblasted stainless steel cup (ST30-4V-40/133 and CC39/S respectively, Anton Paar) was used for all the tests, measuring the torque obtained in a series of decreasing rotational speed steps (from 80 to 1 rpm, 10 s each) after a pre-shear interval (340 s) at 100 rpm. The resulting torque for each measuring step was calculated as mean of the last 5 s of sampled data.

A linear regression for every torque/rotational speed dataset was calculated considering only the data points in the 80–20 rpm rotational speed interval (i.e., in the 14.2–16.3 min interval from the first water–cement contact). The linear regression represents the Bingham model for the given cement paste. This latter was extrapolated to zero rotational speed (i.e., to the ordinate intersect, Figure 3) in order to obtain the Bingham dynamic yield torque  $T_0$  [38].

The relative Bingham dynamic yield torque  $T_R$  was then calculated for each lignin-containing cement paste with the following relation

$$T_R = \frac{T_0}{T_{0,ref}}$$

where  $T_0$  is the obtained Bingham dynamic yield torque and  $T_{0,ref}$  is the yield torque measured with the reference paste (0.45  $w/c$  ratio cement paste without lignin).

The water/cement ratio  $W_L$  at the unit value of  $T_R$  (i.e., at the reference Bingham dynamic yield torque) was calculated for each cement paste with the inverse linear regression of the yield torque/water cement ratio dataset (Figure 4).

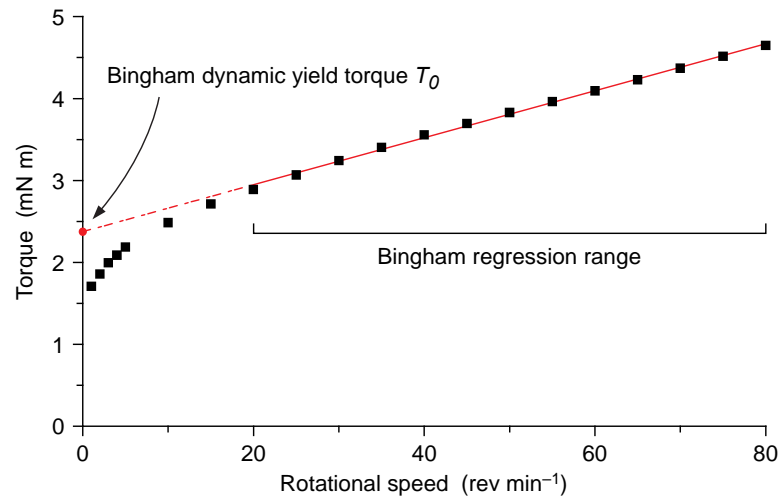


**Figure 3.** Bingham fitting of torque vs. rotational speed data. The Bingham dynamic yield torque  $T_0$  was obtained by extrapolating the Bingham model to zero rotational speed.

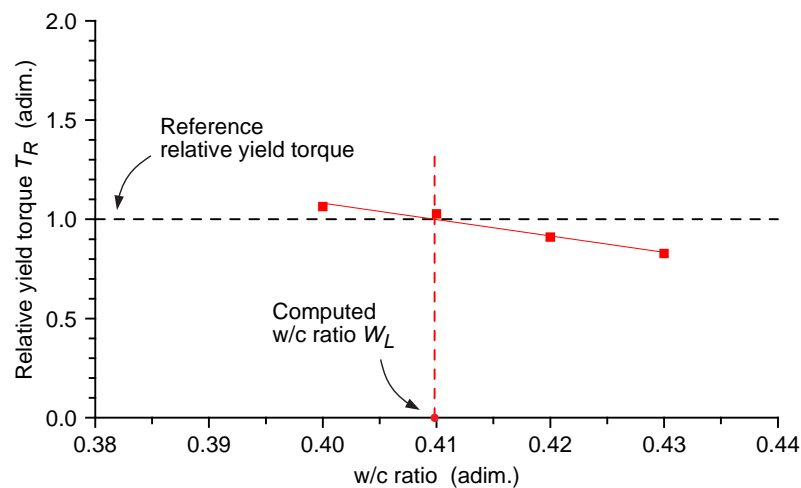


**Figure 4.** Relative dynamic Bingham yield torque vs. water/cement ratio data set for the BSG<sub>T</sub> Lignin cement paste sample and determination of computed  $W_L$ . The Bingham yield torque measured at each  $w/c$  ratio (red squares) was relative to the yield torque of the reference cement paste (without lignin) at 0.45  $w/c$  ratio. The  $W_L$  value obtained with the lignin containing cement paste was calculated intersecting the reference yield torque value (black dotted line) with the sample points data fitting line (red solid line).

The actual water reduction for a given lignin is given by the following relation

$$W_R = 100 \cdot \left( 1 - \frac{W_L}{W_{ref}} \right)$$

where  $W_R$  is the obtained water reduction (%),  $W_L$  is the computed  $w/c$  ratio at the reference yield torque for the given lignin, and  $W_{ref}$  is the reference  $w/c$  ratio (0.45).

This procedure measured the effective water reduction capability of each lignin in the preparation of a cement paste in the given conditions.

### 3. Results and Discussion

#### 3.1. BSG Waste Pre-Treatment and Sugar Process

As mentioned before, BSG waste contains a number of components, of which polysaccharides, proteins, fibers (hemicellulose, cellulose, and lignin), fats and inorganic salts are the most representative ones.

Using water as a solvent, preliminary experiments were performed in order to establish how much starch/polysaccharides could be extracted from untreated BSG (BSG<sub>U</sub>). The results were encouraging because repeated extractions with hot water allowed a considerable reduction of the initial BSG weight (up to 20%). Therefore, a new protocol based on a strong thermic treatment followed by three aqueous extractions was set up, allowing the separation of a relevant amount of soluble materials. Accordingly, dried BSG was ground, suspended in water, and heated in an autoclave (121 °C, 15 min). The solid was filtrated, washed with water, and dried again. Overall, more than 25% of the initial BSG weight was dissolved in water. The obtained solution, enriched in soluble starch, proteins, and other minor nutrients, could be regarded as a valuable growing medium for microbial fermentation. Therefore, a new medium made up of BSG extract (6.8 g/L), yeast extract (1 g/L), and ammonium sulfate (3 g/L) was defined (reported as BSG medium in Figure 1). The addition of yeast extract, even in low amount, is crucial because it provides vitamins and microelements essential to microbial fermentation. In addition, although BSG contains proteins, the nitrogen content of the aqueous extract is not sufficient to ensure good biomass production. Consequently, ammonium sulfate as a suitable nitrogen source was selected. The latter compound is a very cheap chemical, largely employed in industry and in microbiology where it is used to replace peptone or other protein sources. Hence, the new medium was tested for the fermentation of some selected microorganisms. Attention was focused on the evaluation of the strains only belonging to the BL-1, with high preference of those generally recognized as safe for human health (GRAS). In addition, they must be able to metabolize starch/polysaccharides and to produce compounds of commercial interest. More specifically, a preliminary screening allowed us to single out six different microorganisms (Table 1), three fungal and three bacterial strains.

The growth of the strains was tested taking into account the possible scalability to industrial production. Hence, fermentation experiments were performed in a 5 L bioreactor, using at least 1.5 L of BSG medium, with accurate control of the temperature, stirring, and aeration parameters.

The first investigated strain, *Phaffia rhodozyma* [39], is a basidiomycetous yeast that was found in slime fluxes of certain broad-leafed trees. This microorganism takes advantage of its fermentative abilities to use the carbohydrates there present for its growth, thus indicating potential employment in the transformation of other polysaccharide-rich substrates. The most remarkable features of *P. rhodozyma* is its pink-orange color due the production of carotenoid pigments and especially of astaxanthin. This compound has great economical relevance because it is a widely used feed ingredient, utilized for the pigmentation of fish and crustaceans, and is one of the most expensive feed ingredients in the aquaculture industry [40,41]. In addition, the European Commission has authorized the direct use of the whole yeast biomass in foodstuffs for salmon and trout [16], including the use of astaxanthin overproducing strains [42]. Therefore, we tested the biomass productivity of a wild-type strain of *Phaffia rhodozyma* (DSM 5626) using our BSG medium (Table 1, entry 1). As soon as the microorganism reached the stationary phase of growth, the biomass was separated by centrifugation and then was freeze-dried, until complete removal of the water content. Three-point-six grams of dry biomass per liter of BSG medium were obtained, corresponding to a productivity of 135 g of dry yeast per kilogram of dry BSG. These very good results clearly indicated the potential of BSG medium in biomass production and its specific use for the above-described industrial application.

The other five strains reported in Table 1 were selected taking into account their capacity of lipids accumulation. Indeed, the yeast *Yarrowia lipolytica* and the bacterium *Rhodococcus opacus* are well known oleaginous microorganisms, able to produce triglyc-

erides starting from a number of different waste materials as substrates [43,44]. In particular, *Yarrowia lipolytica* is a GRAS microorganism and the European Commission has authorized the commercialization of the dried and heat-killed biomass of all *Y. lipolytica* strains as a novel food ingredient [45]. Moreover, in specific culture condition, this microorganism can produce lipids having a composition resembling that of cocoa butter [46] and has been selected to integrate by fermentation the limited production of this natural fat. In contrast, *Rhodococcus opacus* has not been used for food applications yet. Since this microorganism has the capacity to grow on different kind of substrates, accumulating high level of triglycerides, *R. opacus* has been used for the production of biodiesel from organic wastes [47]. Similarly, strains belonging to the genus *Streptomyces* have been studied for their ability in the degradation of lignocellulose wastes leading to the production of branched chain fatty acid (BCFA) derivatives [48]. These compounds possess a number of physical, chemical, and biological properties. Due to their low melting points, BCFAs esters have been selected as preferred biofuels for use in cold environments, whereas BCFAs show protective activity against neonatal necrotizing enterocolitis (NEC), a potentially lethal disease representing the major cause of morbidity in premature infants [49]. For the latter reason, these compounds have been proposed for inclusion in infant food formulas as human milk fat substitutes [50].

In the context of bacteria degrading lignocellulose wastes, two *Streptomyces* strains were isolated from a soil sample, polluted with cereal and fodder residues. The strains were identified as *Streptomyces cavourensis* and *Streptomyces albidoflavus* and were deposited in DMSZ collection under the numbers DSM 112466 and DSM 112467, respectively.

Both the biomass productivity and the fatty acids productivity of all the above-described fungal and bacterial species, grown on BSG medium, were investigated (Table 1, entry 2–6). As described for *P. rhodozyma*, the biomass was separated by centrifugation as soon as the microorganism reached the stationary phase of growth, freeze-dried, completely hydrolyzed, and analyzed by GC–MS after acidification and extraction as reported in Section 2.4 (Table 2).

**Table 2.** Fatty acid composition of the glycerides produced by the selected microbial strains grown in BSG medium.

Microbial Strain	Branched Chain FAs (%) <sup>1</sup>			Linear FAs (%) <sup>1</sup>			Undetermined FAs (%) <sup>1,2</sup>
	<i>iso</i>	<i>anteiso</i>	Others	SFAs <sup>3</sup>	MUFAs <sup>4</sup>	PUFAs <sup>5</sup>	
<i>Yarrowia lipolytica</i> (DSM 70562)	-	-	-	16.5	9.0	72.0	2.5
<i>Rhodococcus opacus</i> (DSM 43205)	-	-	4.0 <sup>6</sup> ; 15.1 <sup>7</sup>	44.6	21.7	9.1	5.5
<i>Streptomyces cavourensis</i> (DSM 112466)	28.4	37.7	6.8 <sup>6</sup>	15.0	3.7	7.5	0.9
<i>Streptomyces albidoflavus</i> (DSM 112467)	18.6	39.1	8.1 <sup>6</sup>	15.2	7.0	5.8	6.2

<sup>1</sup> The percentages are determined by GC–MS analysis of the crude fatty acids mixture derivatized as methyl ester derivatives. <sup>2</sup> The percentage indicates the sum of the fatty acids whose chemical structure was not determined. <sup>3</sup> Saturated fatty acids. <sup>4</sup> Monounsaturated fatty acids. <sup>5</sup> Polyunsaturated fatty acids. <sup>6</sup> The percentage indicates the sum of the fatty acids possessing a cyclopropyl ring in their chemical framework. <sup>7</sup> Percentage of 10-methyl-octadecanoic acid (tubercolostearic acid).

The two *Yarrowia lipolytica* strains, DSM 8218 and DSM 70562, were isolated from very different environments, namely from a diesel fuel tank and from marzipan, respectively. Despite this fact, they showed similar characteristics both in term of biomass and fatty acid productivity (Table 1, entry 2 and 3). The dry yeast was obtained in yield of about 1.5 g and 1.6 g per liter of BSG medium respectively, whereas the oil production ranged from 200 mg to 220 mg of isolated fatty acid per liter of BSG, respectively.

Otherwise, *Rhodococcus opacus* DSM 43205 showed better performances. The fermentation afforded 2.4 g of dry biomass per liter of BSG medium, yielding 547 g/L of isolated

fatty acids (Table 1, entry 3). Finally, the two *Streptomyces* strains showed results comparable to those obtained with *Y. lipolytica* strains, with *S. cavourensis* showing slightly higher productivity (2.1 g/L biomass and 220 mg/L of FAs) than *S. albidoflavus* (1.7 g/L biomass and 180 mg/L of FAs).

The most relevant differences among the investigated fungal and bacterial species were highlighted by the GC–MS analysis of the fatty acids mixtures isolated from the corresponding biomasses (Table 2). In more detail, *Y. lipolytica* contained only linear FAs, of which 72% corresponded to polyunsaturated fatty acids (PUFAs), mainly made up of linoleic acid. In contrast, the bacterium *R. opacus* produced predominantly saturated fatty acids (SFAs), although monounsaturated fatty acids (MUFAs), PUFAs, and some specific BCFAs, such as cyclopropane containing FAs and 10-methyl-octadecanoic acid, were present.

The two *Streptomyces* species showed very similar fatty acid composition. Both microorganisms accumulated prevalently BCFAs and the majority of the fatty acid mixture was made up of *iso*- and *anteiso*-fatty acids.

Overall, the present study outlines four possible applications of the BSG<sub>T</sub> medium. Fermentation of *P. rhodozyma* and *Y. lipolytica* could afford biomass materials to be employed in aquaculture and human alimentation, respectively. Moreover, *R. opacus* and *S. cavourensis* could provide the FA derivatives useful for the preparation of different kinds of biodiesel and for the formulations of the BCFA-containing human milk fat substitutes, respectively.

### 3.2. Lignocellulose Process

#### 3.2.1. DES-Mediated Fractionation

Recently, some innovative biomass DES-based treatments have been reported in the literature in the context of exploiting agricultural waste in biorefineries [51–53]. However, the described treatments were mainly focused on the obtainment of a high quantity of fermentable sugars as in the majority of the research concerning biomass exploitation [54]. In this work, a new protocol of biomass DES-based treatment coupled with the previous sugar process step (described in Section 3.1) has been set up with the special aim of lignin recovery and exploitation.

Different DESs were prepared by heating and stirring the two components, a hydrogen bond acceptor (HBA) and a hydrogen bond donor (HBD), in a defined molar ratio. The quaternary ammonium salts choline chloride (ChCl) and betaine glycine (BetG) were used as HBAs whereas formic acid, acetic acid, and L-lactic acid constituted HBDs, as reported in Table 3.

**Table 3.** List, composition, density (measured at 18 °C) of prepared DESs and data of mass recovery of BSG<sub>U</sub> Cellulose and BSG<sub>U</sub> Lignin (ns represents no separation).

Composition DES HBA/HBD	Molar Ratio (HBA/HBD)	Density of Pure DES (g/cm <sup>3</sup> )	BSG <sub>U</sub> Cellulose Recovery (% w/w Biomass)	BSG <sub>U</sub> Lignin Recovery (% w/w Biomass)
Choline chloride/Formic acid	1/2	1.147	ns	ns
Choline chloride/Acetic acid	1/2	1.103	39	7
Choline chloride/L-Lactic acid	1/5	1.184	25	10
Betaine Glycine/Formic acid	1/2	1.161	55	9
Betaine Glycine/Acetic acid	1/2	1.107	32	8
Betaine Glycine/L-Lactic acid	1/5	1.203	53	7

DESs were prepared using a defined protocol, which consisted of mixing the components in a defined ratio (reported in Table 3) and heating them, under constant stirring, at 90 °C for 2–5 h until a stable, homogeneous, colorless single-phase liquid was formed. The obtained mixtures were dried at reduced pressure for 24 h, preserved under argon, and characterized by <sup>1</sup>H NMR spectra. The final mixtures were then conserved in a desiccator in presence of calcium chloride until a constant weight was observed. The densities of DESs were also measured because these data provided important information about the intermolecular forces that occur during DES formation. Typically, DESs show higher

density than water and the value depends strongly on the type of the HBD and its molar ratio on HBA.

When the BSG was received from the brewery, it was promptly dried for 24 h, finely milled and labeled as BSG<sub>U</sub> (untreated BSG). BSG<sub>U</sub> was suspended in DES at 130 °C under magnetic stirring for 24 h. Then ethanol was gradually added in order to precipitate the BSG<sub>U</sub> Cellulose fraction, which was separated with yields reported in Table 3 (as *w/w* initial biomass). The filtrate was then concentrated and treated with water as anti-solvent to induce lignin precipitation. After centrifugation, filtration, and solvent evaporation the final solid fraction (BSG<sub>U</sub> Lignin) was recovered with a final yield reported in Table 3. The choline chloride/L-lactic acid 1/5 appeared to be the best DES for the treatment of BSG biomass in terms of solubilization of the starting biomass as well as for the handling of the solutions during the DES treatment, and due to the yields of BSG<sub>U</sub> Cellulose and BSG<sub>U</sub> Lignin. For that reason, the present study has focused only on the use of the DES choline chloride/L-lactic acid 1/5 for the lignocellulose fractionation.

From the lignocellulose process point of view, the sugar process (Section 3.1) can be considered as a pretreatment of the waste BSG biomass. The sugar process had the effect of improving the successive lignocellulosic fractionation, enhancing the yields of the two fractions, probably because of better interaction between the solvent and the biomass. Moreover, the reduction of the biomass weight derived from the sugar process allowed, if compared to BSG<sub>U</sub> fractionation, a substantial saving accounting for around 25%, in terms of DES quantity and solvent volumes. This enables a great improvement of the overall process both in economic and environmental terms. In that case, the yield of BSG<sub>T</sub> Cellulose recovery accounted for 40% (instead of 25%) and up to 15% for BSG<sub>T</sub> Lignin instead of 9%.

The ability to recycle DES in a cyclic process would add value to the previous considerations, allowing further potential optimization of the entire process. In this study, a preliminary assessment of the recyclability of DES was conducted by performing a series of three successive treatments recycling the DES after precipitation of the BSG<sub>T</sub> Lignin without further purification apart from water evaporation. This study demonstrated a quite good preservation of the DES (by NMR analysis, Supplementary Materials Figure S2) and a substantial conservation of yields indicating a great potential to configure the lignocellulosic process as a closed loop with respect to DES.

### 3.2.2. BSG<sub>T</sub> Lignin Characterization

A deep characterization was carried out on the recovered BSG<sub>T</sub> Lignin using as reference a well known commercial soda lignin (Protobind 1000, indicated from now on as Protobind).

#### Solvent Solubilization Determination

Solubilization studies are a key step in lignin characterization and valorization. In fact, one of the main drawbacks currently hampering effective lignin exploitation is generally its poor solubility in aqueous systems and in the most commonly used organic solvents. In order to determine the solubility characteristics of the present recovered BSG<sub>T</sub> and BSG<sub>U</sub> Lignins, a solubilization study was performed with water and six organic solvents: *n*-butyl acetate (BuOAc), ethyl acetate (EtOAc), 2-butanone (MEK), methanol (MeOH), *tert*-butyl methyl ether (MTBE), and tetrahydrofuran (THF). The resulting extraction yields (as *w/w* percentage of solubilized fraction vs. total fraction) are reported in Figure 5 (with water solubility as the comparison). For a better evaluation, the data for the commercial lignin Protobind have been also recorded and inserted in Figure 5.

Like Protobind, the two BSG lignins (BSG<sub>U</sub> and BSG<sub>T</sub> Lignins) were quite insoluble in water, but on the other hand were soluble in the selected organic solvents; showing, however, a general lower solubility when compared to Protobind in all tested organic solvents. MEK, methanol, and THF appeared to be the best choices for the solubilization of these lignins with a range of solubility from 32–35% for BSG<sub>U</sub> Lignin and 40–56% for

BSG<sub>T</sub> Lignin. Moreover, it is clear from the Figure 5 that BSG<sub>T</sub> Lignin always presented a higher solubility than BSG<sub>U</sub> Lignin in the examined solvents: in THF the solubility was 25% higher, in MEK 45%, and in MeOH 61%. This characteristic constitutes a great advantage in further potential lignin exploitation.

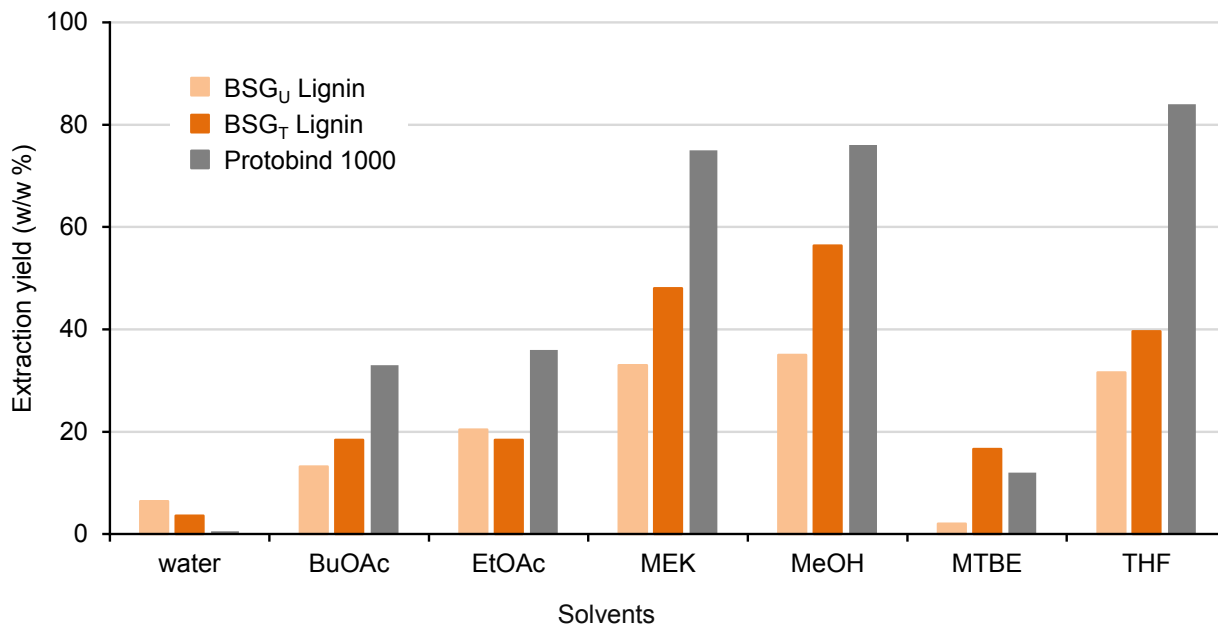


**Figure 5.** Extraction yield of a commercial technical lignin (Protobind) and the two lignins extracted from BSG (BSG<sub>U</sub> and BSG<sub>T</sub> Lignins). The data are reported as the percentage (*w/w*) of solubilized fraction vs. total fraction in 6 different organic solvents and water.

#### GPC Results

The molecular weight and the molecular weight distribution of the lignin samples were determined by means of GPC. In Table 4, the number average molecular weight ( $M_n$ ), the weight average molecular weight ( $M_w$ ), and the polydispersity index ( $\mathcal{D}$ ) of BSG lignins and Protobind, used as benchmark, are reported. As can be seen, the lignocellulose process led to BSG lignin fractions characterized by a lower molecular weight and lower  $\mathcal{D}$  compared to Protobind. In particular, a slightly lower  $M_n$  was observed in BSG<sub>T</sub> Lignin, likely resulting from the isolation method (aqueous extraction), which may lead to an enrichment of low-molecular-weight fractions. This also leads to a slightly higher  $\mathcal{D}$ . In contrast, no significant differences between BSG<sub>T</sub> and BSG<sub>U</sub> Lignins were observed in terms of  $M_w$ .

**Table 4.** Number average molecular weight ( $M_n$ ), weight average molecular weight ( $M_w$ ), and polydispersity index ( $\mathcal{D}$ ) of all examined lignins (samples were eluted after acetylation; reported values are relative to polystyrene standards).

Sample	$M_n$ (g/mol)	$M_w$ (g/mol)	$\mathcal{D}$
BSG <sub>U</sub> Lignin	820	1580	1.93
BSG <sub>T</sub> Lignin	670	1630	2.43
Protobind 1000	830	2800	3.37

#### Sugars Quantification

The total reducing sugar quantification in the final BSG<sub>U</sub> and BSG<sub>T</sub> Lignins was performed using the bincinconic assay method with some modifications (see Section 2.8). It was necessary to set two different calibration curves, a and b (respectively reported in Supplementary Materials Figures S3 and S4), established by using glucose solutions in the 0–80  $\mu$ M concentration range as standards. In particular, the calibration curve a was

used to evaluate the sugar content of samples soluble in water, and the calibration curve b for samples insoluble in water, but soluble in dimethylsulfoxide (DMSO). Curve a was used to analyze aqueous sugar solutions after step 2 (BSG<sub>T</sub> medium filtrate) whereas curve b, recorded for DMSO soluble samples, was used to analyze lignins and lignin samples subjected to acid hydrolysis. This procedure was conducted to evaluate the presence of complex saccharides in lignins. The results for BSG<sub>U</sub> and BSG<sub>T</sub> Lignins are reported in Table 5, as well as the data for Protobind. The reducing sugars in the BSG lignins appeared to be around 0.20% (*w/w*), lower than the value in Protobind (~0.34%), with a reduction for BSG<sub>T</sub> Lignin that demonstrated that the sugar process is quite effective for the recovery of a higher-quality lignin. Furthermore, after hydrolysis, Protobind showed also the presence of a higher quantity (13%) of complex sugars, whereas in these conditions, for the two BSG lignins this amount was much lower. This result is fundamental in view of the applications of these lignins in the development of cement water reducers.

**Table 5.** Results of the total reducing sugar quantification.

Sample	Reducing Sugars/Biomass ( <i>w/w</i> )	Reducing Sugars/Biomass after Hydrolysis ( <i>w/w</i> )
BSG <sub>U</sub> Lignin	0.25%	2.9%
BSG <sub>T</sub> Lignin	0.18%	3.3%
Protobind 1000	0.34%	13%

#### Phenolic Hydroxyl Group Determination

The total phenolic content in the recovered BSG<sub>U</sub> and BSG<sub>T</sub> Lignins was determined using the Folin–Ciocalteu (FC) assay. The test is based on the reaction of phenolic hydroxyl groups with a specific redox reagent (FC reagent), which leads to the formation of a blue chromophore, which is, however, sensitive and unstable in strong bases. Therefore, based on an analytical protocol previously demonstrated by our group [55], DMSO was used as solvent for the samples in order to obtain their complete solubilization in neutral conditions. The phenolic content results are reported in Table 6 as vanillin equivalents (mmol/g of dry lignin) with the data for Protobind as a reference.

**Table 6.** Results of the determination of phenolic hydroxyl groups expressed as vanillin equivalents/g of lignin sample. Estimated standard errors  $\pm 0.2$  mmol/g vanillin equivalent (1  $\sigma$ , from calibration data).

Sample	Vanillin Equivalent Content (mmol/g)
BSG <sub>U</sub> Lignin	1.1
BSG <sub>T</sub> Lignin	1.2
Protobind 1000	3.1

BSG<sub>U</sub> and BSG<sub>T</sub> Lignins show a quite similar content of vanillin equivalents (around  $1.15 \pm 0.05$ ), which is nearly half the amount value if compared to Protobind. The trend seemed to be confirmed by <sup>31</sup>P NMR analysis as will be illustrated later in the text. The quite similar values of the two BSG lignins demonstrated that the pretreatment carried out in the sugar process has no influence on phenolic functionalities.

#### Total Hydroxyl Groups Quantification by <sup>31</sup>P NMR

The different hydroxyl groups present in the recovered BSG lignins were deeply investigated by <sup>31</sup>P NMR. The spectra are shown in Figure 6, where Protobind has been also recorded for a comparison.

In detail, three sections of the spectra were analyzed and integrated to perform the attribution of the different hydroxyl groups: the signals from 150–147 ppm are associated to the aliphatic hydroxyl groups, the signals from 145–138 ppm represent the signals associated with aromatic hydroxyl groups, whereas the signals centered on 136 ppm account for the carboxylic acid residues. The peak integration in these three parts of

the spectra led to the quantification of the total hydroxyl groups expressed in mmol of functional group per g of dry lignin, as reported in Table 7 below.

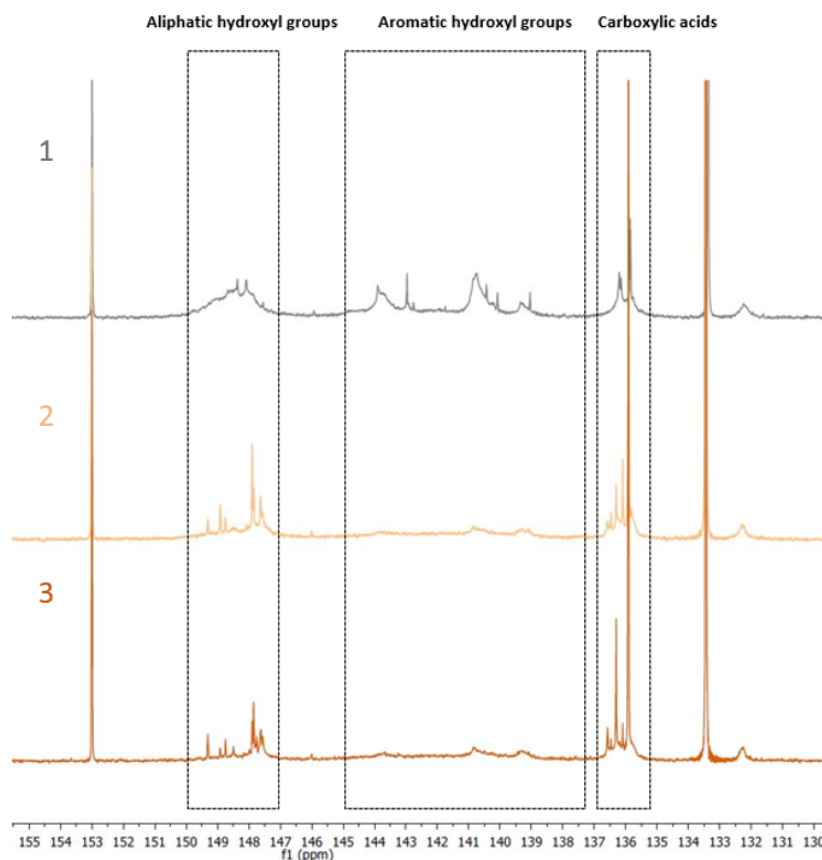


**Figure 6.** <sup>31</sup>P NMR spectra of Protobind 1000 (spectrum 1 in gray), BSG<sub>U</sub> Lignin (spectrum 2 pale orange), BSG<sub>T</sub> Lignin (spectrum 3 dark orange).

**Table 7.** Detailed hydroxyl/carboxyl quantification by <sup>31</sup>P NMR (as mmol of functional group per g of dry lignin).

Sample	-OH Aliphatic (mmol/g)	-OH Aromatic (mmol/g)	-COOH (mmol/g)
BSG <sub>U</sub> Lignin	2.27	2.77	2.30
BSG <sub>T</sub> Lignin	1.78	3.21	3.99
Protobind 1000	3	4.67	1.42

Lignins from BSG seemed to show a higher concentration of carboxylic residues but a lower quantity of aliphatic and aromatic hydroxyl functionalities if compared with Protobind. In particular, it appears very interesting that BSG<sub>T</sub> Lignin presented a higher quantity of aromatic OH and carboxylic functionalities when compared to the other samples, which could be a very important tool for the investigation of its use in the preparation of lignin-based macromolecular materials where the presence of such functionalities are mandatory. More specifically, target applications for this lignin fraction may include the field of phenolic resins and adhesives and the field of epoxy-based systems for fiber-reinforced composite materials.

#### Fourier-Transform Infrared Spectroscopy

FT-IR spectroscopy was carried out with the aim of studying the chemical composition of the extracted BSG lignins. The spectrum of Protobind is also presented for comparison purposes. The results obtained are reported in Figure 7, where a zoom of the

fingerprint region is also presented. All three lignins showed a broad absorption band in the region 3400–3200  $\text{cm}^{-1}$ , attributed to the stretching vibrations of the aliphatic and phenolic O-H groups, and three distinct signals in the region 3050–2800  $\text{cm}^{-1}$  related to C-H bond stretching in methyl and methylene groups. The region from 1740 to 1710  $\text{cm}^{-1}$  is attributable to the stretching vibration of C=O in unconjugated ketones, carbonyl, and ester groups [38,55]. Within this region, the signal located at 1710  $\text{cm}^{-1}$  is visible in all lignin spectra, whereas the signal located at 1740  $\text{cm}^{-1}$  is found only in the cases of BSG lignins (blue arrows). This additional signal can be associated with the higher concentration of C=O moieties from carbohydrate origin contained in the two extracted lignins, which is an indication of the slightly lower purity of the BSG lignins compared to Protobind. In the case of BSG<sub>U</sub> Lignin, a signal is clearly detectable at 1660  $\text{cm}^{-1}$ , likely attributable to conjugated carbonyl/carboxyl stretching. This signal confirms the presence of the highest concentration of C=O moieties (*viz.*, of carbohydrates species) in the lignin recovered from the untreated biomass [56]. The bands ascribable to the aromatic skeletal vibrations in lignin are located at 1600  $\text{cm}^{-1}$ , 1515  $\text{cm}^{-1}$ , 1463  $\text{cm}^{-1}$ , and 1430  $\text{cm}^{-1}$  (the last one barely visible in BSG lignins) in all the three lignin samples. Among these, the two signals at 1463  $\text{cm}^{-1}$  and 1430  $\text{cm}^{-1}$  derive from the combination of aromatic ring vibration and C-H deformation [56,57]. Below 1430  $\text{cm}^{-1}$ , the interpretation of bands becomes more difficult, since the signals are given by complex contributions from different vibrational modes. In more detail, aliphatic O-H group vibrations combined with stretching vibrations of aliphatic C-H in methyl groups were found at around 1370  $\text{cm}^{-1}$  in all lignins. Only in the case of Protobind was a further signal at 1330  $\text{cm}^{-1}$  attributable to the syringyl ring breathing found. At 1270  $\text{cm}^{-1}$  and 1217  $\text{cm}^{-1}$ , two peaks associated with C-O vibration in aromatic rings of G-units combined with C=O stretching and C-C, C-O and C=O stretching, respectively, were detected. It is noteworthy that the broadening of these two peaks in both BSG lignins together with the absence of the syringyl ring breathing signal is consistent with the predominant content of guaiacyl units expected in BSG lignins, as reported in the literature [56,58]. At 1120  $\text{cm}^{-1}$  a band associated with CH in-plane deformation in S-units was observable in all cases (more evidently in Protobind), while only in Protobind was the absorption signal at 1153  $\text{cm}^{-1}$  related to C=O deformations in conjugated ester groups of G/S/H units visible. In addition to these, signals associated with aromatic C-H in-plane deformation (typical for S-units), secondary alcohols, and C=O stretching were observed in all spectra collected in the region from 1130  $\text{cm}^{-1}$  to 1120  $\text{cm}^{-1}$ . The shoulder at around 1090  $\text{cm}^{-1}$  appearing in all three lignins can be associated with C-O deformations in secondary alcohols and aliphatic ethers [56].

In general, FT-IR results indicated a good match between the chemical structure of the BSG lignins and that of Protobind. The minor differences found between the recovered lignins and the reference system are likely attributable to the lower level of purity of the BSG<sub>U</sub> Lignin (higher carbohydrates content) and the large number of G-units in both BSG lignins.

#### Differential Scanning Calorimetry

The thermal transitions of the recovered lignins were assessed by DSC analysis. As shown in the DSC scans reported in Figure 8, the glass transition temperature ( $T_g$ ) for both BSG lignins was found to be higher compared to the  $T_g$  of the reference Protobind. In line with the outcomes of  $^{31}\text{P}$ -NMR analysis, this trend may be associated with the higher content of carboxylic groups found in BSG lignins vs. Protobind, which are likely to yield increased hydrogen bonding interactions between the macromolecular chains, ultimately leading to reduced macromolecular mobility and thus increased  $T_g$ . In more detail,  $T_g$  of BSG<sub>T</sub> Lignin is found at a slightly higher temperature than that of BSG<sub>U</sub> Lignin. In this case, this evidence also appears in line with the higher content of -OH aromatic functionalities and carboxyl groups in this treated lignin fraction vs. the untreated counterpart. The value of  $T_g$  is of fundamental importance in lignin valorization, especially in the field of material

science and engineering, where high temperature processing is often encountered. In this context, a higher T<sub>g</sub> value can be an advantage in those applications that require a good thermal stability of the material, such as in the case of thermosets and composites.

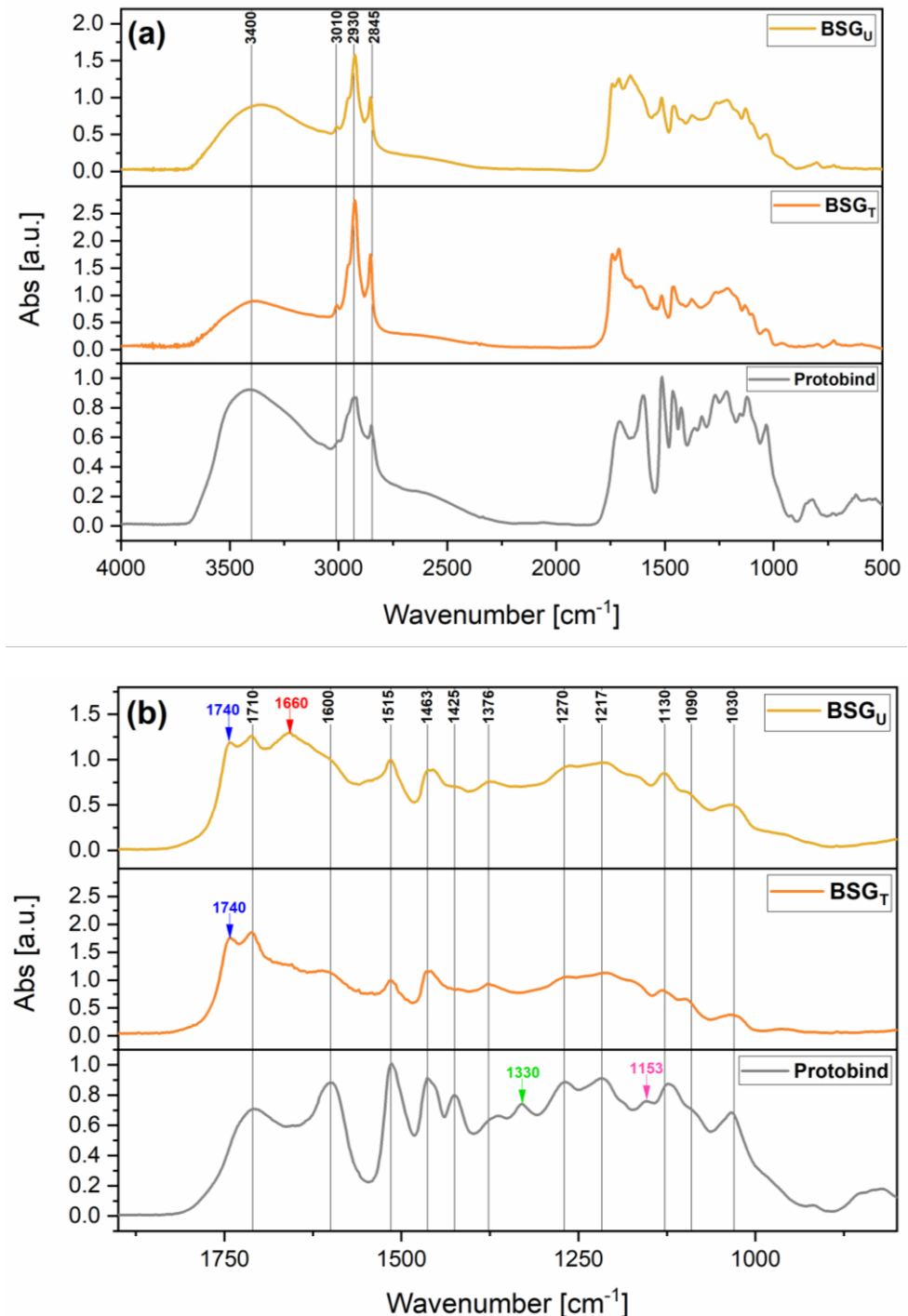


**Figure 7.** (a) FT-IR spectra of BSG<sub>U</sub> Lignin, BSG<sub>T</sub> Lignin, and Protobind; (b) zoomed view of the fingerprint region.

### 3.2.3. Water Reduction in Cement Pastes

Albeit several lignosulfonates are used directly as low-performance cement plasticizers, natural lignins are very interesting as a basis for the development of sustainable superplasticizers through different types of derivatization. These include, among others, oxidation [33], sulfomethylation [59], and grafting with various polymers such as PEG [60],

acrylates [61], and sulphanilic acid-phenol-formaldehyde condensates [62]. Although lignosulfonates typically demonstrate better water reduction properties than natural lignins, the latter have been successfully adopted in several studies as a starting point in the development of experimental high-performance plasticizers for cement, both with a specific sulfonation step [34] and without sulfonation at all [33]. The use of DES fractionation methods results in the production of an underivatized lignin that is comparable to lignins obtained with mild lignocellulosic fractionation methods such as the organosolv or soda processes. The obtained water reduction capabilities of BSG<sub>T</sub> Lignin, BSG<sub>U</sub> Lignin, and Protobind (Section 2.9) are reported in Figure 9.

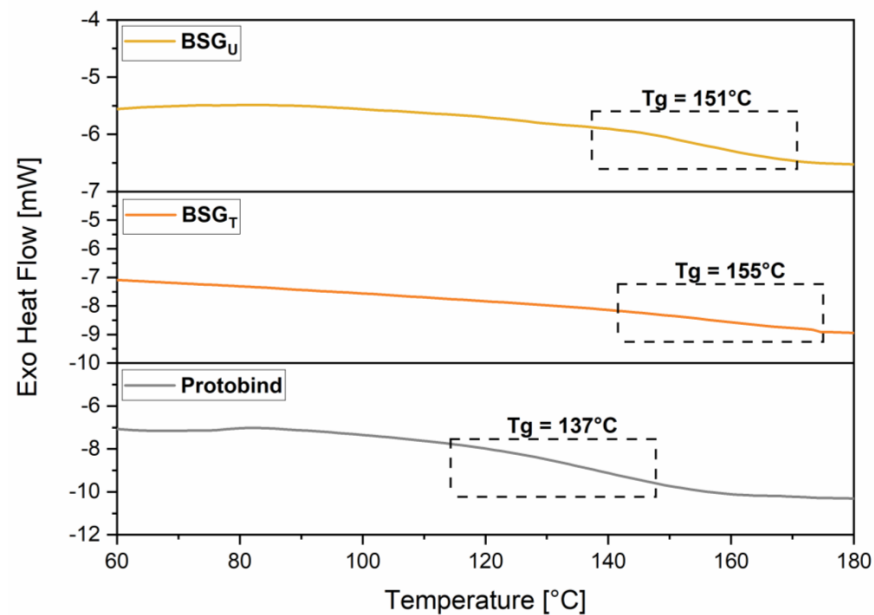


Figure 8. DSC curves of BSG<sub>U</sub> Lignin, BSG<sub>T</sub> Lignin, and Protobind 1000.

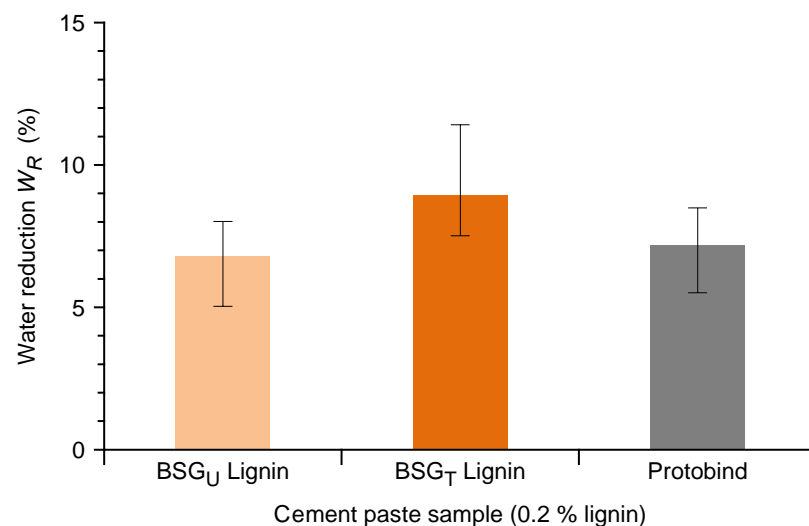


Figure 9. Measured water reduction capability for cement pastes containing 0.2% BSG<sub>U</sub> Lignin, BSG<sub>T</sub> Lignin, and Protobind. Error bars show confidence interval (95%) of the inverse linear regression.

The measurements were carried out using cement pastes (blends of water and cement powder) that are a quite simpler system in comparison with concrete (blends of water, cement powder, sand, and aggregates) or even mortars (blends of water, cement powder, and sand). This allowed performing the required tests with very low sample volume (about 100 mL) and thus with very little quantity of lignin. The applied procedure allows direct measurement of the water reduction capability of each lignin, keeping constant

a specific rheological parameter (the Bingham dynamic yield torque, which estimates the minimum torque needed to maintain an established flow in the given experimental conditions), and it was thus considered a good indication of the potential performance of the lignins in the final system (concrete). The measurements demonstrate a fairly comparable water reduction capability for the BSG<sub>T</sub> and the BSG<sub>U</sub> Lignins. Moreover, both lignins demonstrate a water reduction capability substantially equivalent to the commercial soda lignin Protobind. This is a good indication that the proposed process, and more generally the DES based fractionation process, is capable of producing a lignin with water reduction capability comparable to a typical industrial soda lignin. Moreover, BSG<sub>T</sub> Lignin demonstrated a quite high content of carboxylic and aromatic hydroxylic residues that are exploitable in several derivatization methods. These results suggest that the lignin obtained in the described process is suitable to constitute the basis for the development of a high-performance, sustainable lignin-based water reducer for the production of concrete.

#### 4. Conclusions

In this work, we described in detail a process (reported in Figure 2), which started from wet BSG recovered from a regional brewery and ended with the production of different compounds of industrial interest. Overall, the presented research reports on the almost complete transformation and exploitation of the starting BSG waste. A comprehensive approach combining biomass hot water treatment with successive deep eutectic solvent-mediated fractionation was developed in order to maximize the process versatility. The upstream phase, which provided an aqueous solution called BSG medium, allowed us to exploit the soluble moiety (which accounted  $\approx 35\%$ , *w/w*) composed of proteins and soluble sugars, as a fermentation medium with high yields of different microorganisms leading to the production of linear and branched chains fatty acids. The solid outcome of the upstream phase underwent fractionation mediated by deep eutectic solvents. A subsequent precipitation firstly with ethanol and then with water provided two main products, BSG<sub>T</sub> Cellulose and a BSG<sub>T</sub> Lignin, with a final yield of 30% and 10%, respectively. This lignin has been fully characterized in terms of its chemical, physical, thermal, and structural properties. Moreover, BSG<sub>T</sub> Lignin has then been tested as water reducer in cement paste with comparable results to technical commercial soda lignin, indicating that it can constitute a good basis for the development of sustainable water reducers for concrete. Overall, our study proposed an integrated multistep fractionation process that could enhance the perspectives of recyclability of BSG. Accordingly, around 75–80% of the mass of the latter important agrofood waste is transformed into high-value-added products of industrial relevance. These results, even in their preliminary form, fulfill the principles of circular economy and give new insights in the field of the biotransformation of agrofood wastes.

**Supplementary Materials:** The following supporting information can be downloaded at: <https://www.mdpi.com/article/10.3390/fermentation8040151/s1>, Figure S1. <sup>1</sup>H NMR spectrum of DES choline chloride/L-lactic acid (1:5 mol/mol); Figure S2. <sup>1</sup>H NMR spectrum of DES choline chloride/L-lactic acid (1:5 mol/mol) after recycling; Figure S3. Calibration curve a for glucose quantification registered in H<sub>2</sub>O; Figure S4. Calibration curve b for glucose quantification registered in DMSO; Figure S5. Calibration curve of Folin–Ciocalteu phenol titration with vanillin.

**Author Contributions:** Conceptualization, P.D., S.S., A.S., and D.T.; methodology, P.D., A.S., L.S., S.S.; investigation, C.A., E.B., G.G., S.M., L.A.M.R., E.R., S.S., A.S.; resources, P.D., G.G., S.S., A.S., S.T.; writing—original draft preparation, P.D., G.G., S.S., A.S., D.T.; writing—review and editing, C.A., P.D., G.G., L.A.M.R., S.S., A.S., E.R., D.T., S.T.; funding acquisition, P.D., G.G., S.S., S.T. All authors have read and agreed to the published version of the manuscript.

**Funding:** This research project has been partially funded by Regione Lombardia and Fondazione Cariplo (grant number 2018-1739, project: POLISTE) and by the European Union's Horizon 2020 Research and Innovation Programme (grant Agreement no. 952941, project: BIOMAC). L.R. is a Ph.D.

student of the Research Doctorate Program in Chemical Engineering and Industrial Chemistry at Politecnico di Milano.

**Data Availability Statement:** Data are contained within the article and Supplementary Materials.

**Acknowledgments:** The authors gratefully acknowledge Professor Francesco Gatti (Politecnico di Milano) for his valuable help in the setup of NMR experiments. The authors also thank the Brewery “L’Orso Verde” for providing BSG.

**Conflicts of Interest:** The authors declare no conflict of interest.

## References

1. *A New Circular Economy Action Plan for a Cleaner and More Competitive Europe*; COM(2020) 98; European Commission, Directorate-General for Environment: Brussels, Belgium, 2020.
2. Mussatto, S.I.; Dragone, G.; Roberto, I.C. Brewers’ spent grain: Generation, characteristics and potential applications. *J. Cereal Sci.* **2006**, *43*, 1–14. [[CrossRef](#)]
3. Thomas, K.; Rahman, P. Brewery wastes. Strategies for sustainability. A review. *Asp. Appl. Biol.* **2006**, *80*, 1–11.
4. Kerby, C.; Vriesekoop, F. An overview of the utilisation of brewery by-products as generated by british craft breweries. *Beverages* **2017**, *3*, 24. [[CrossRef](#)]
5. Buffington, J. The economic potential of brewer’s spent grain (bsg) as a biomass feedstock. *Adv. Chem. Eng. Sci.* **2014**, *4*, 308–318. [[CrossRef](#)]
6. Salihu, A.; Bala, M. Brewer’s spent grain: A review of its potentials and applications. *Afr. J. Biotechnol.* **2011**, *10*, 324–331.
7. Robertson, J.; I’Anson, K.; Treimo, J.; Faulds, C.; Brocklehurst, T.; Eijsink, V.; Waldron, K. Profiling brewers’ spent grain for composition and microbial ecology at the site of production. *LWT Food Sci. Technol.* **2010**, *43*, 890–896. [[CrossRef](#)]
8. Wen, C.; Zhang, J.; Duan, Y.; Zhang, H.; Ma, H. A mini-review on brewer’s spent grain protein: Isolation, physicochemical properties, application of protein, and functional properties of hydrolysates. *J. Food Sci.* **2019**, *84*, 3330–3340. [[CrossRef](#)]
9. He, Y.; Kuhn, D.D.; Ogejo, J.A.; O’Keefe, S.F.; Fraguas, C.F.; Wiersema, B.D.; Jin, Q.; Yu, D.; Huang, H. Wet fractionation process to produce high protein and high fiber products from brewer’s spent grain. *Food Bioprod. Process.* **2019**, *117*, 266–274. [[CrossRef](#)]
10. Martínez-Avila, O.; Llenas, L.; Ponsá, S. Sustainable polyhydroxyalkanoates production via solid-state fermentation: Influence of the operational parameters and scaling up of the process. *Food Bioprod. Process.* **2022**, *132*, 13–22. [[CrossRef](#)]
11. de Crane d’Heysselaer, S.; Bockstal, L.; Jacquet, N.; Schmetz, Q.; Richel, A. Potential for the valorisation of brewer’s spent grains: A case study for the sequential extraction of saccharides and lignin. *Waste Manag. Res.* **2021**, 734242X211055547. [[CrossRef](#)]
12. Outeiriño, D.; Costa-Trigo, I.; Pinheiro de Souza Oliveira, R.; Pérez Guerra, N.; Domínguez, J.M. A novel approach to the biorefinery of brewery spent grain. *Process Biochem.* **2019**, *85*, 135–142. [[CrossRef](#)]
13. Parchami, M.; Ferreira, J.A.; Taherzadeh, M. Brewing process development by integration of edible filamentous fungi to upgrade the quality of brewer’s spent grain (bsg). *Bioresources* **2021**, *16*, 1686–1701. [[CrossRef](#)]
14. Dursun, D.; Koulouris, A.; Dalgıç, A.C. Process simulation and techno economic analysis of astaxanthin production from agro-industrial wastes. *Waste Biomass Valoriz.* **2020**, *11*, 943–954. [[CrossRef](#)]
15. Caporusso, A.; Capece, A.; De Bari, I. Oleaginous yeasts as cell factories for the sustainable production of microbial lipids by the valorization of agri-food wastes. *Fermentation* **2021**, *7*, 50. [[CrossRef](#)]
16. Gillet, S.; Aguedo, M.; Petitjean, L.; Morais, A.R.C.; Lopes, A.M.D.; Lukasik, R.M.; Anastas, P.T. Lignin transformations for high value applications: Towards targeted modifications using green chemistry. *Green Chem.* **2017**, *19*, 4200–4233. [[CrossRef](#)]
17. Collins, M.N.; Nechifor, M.; Tanasa, F.; Zanoaga, M.; McLoughlin, A.; Strozyk, M.A.; Culebras, M.; Teaca, C.A. Valorization of lignin in polymer and composite systems for advanced engineering applications—A review. *Int. J. Biol. Macromol.* **2019**, *131*, 828–849. [[CrossRef](#)] [[PubMed](#)]
18. Tribot, A.; Amer, G.; Abdou Alio, M.; de Baynast, H.; Delattre, C.; Pons, A.; Mathias, J.-D.; Callois, J.-M.; Vial, C.; Michaud, P.; et al. Wood-lignin: Supply, extraction processes and use as bio-based material. *Eur. Polym. J.* **2019**, *112*, 228–240. [[CrossRef](#)]
19. Iravani, S.; Varma, R.S. Greener synthesis of lignin nanoparticles and their applications. *Green Chem.* **2020**, *22*, 612–636. [[CrossRef](#)]
20. de Baynast, H.; Tribot, A.; Niez, B.; Audonnet, F.; Badel, E.; Cesar, G.; Dussap, C.-G.; Gastaldi, E.; Massacrier, L.; Michaud, P.; et al. Effects of kraft lignin and corn cob agro-residue on the properties of injected-moulded biocomposites. *Ind. Crop. Prod.* **2022**, *177*, 114421. [[CrossRef](#)]
21. Moreno, A.; Sipponen, M.H. Lignin-based smart materials: A roadmap to processing and synthesis for current and future applications. *Mater. Horiz.* **2020**, *7*, 2237–2257. [[CrossRef](#)]
22. de Haro, J.C.; Allegretti, C.; Smit, A.T.; Turri, S.; D’Arrigo, P.; Griffini, G. Biobased polyurethane coatings with high biomass content: Tailored properties by lignin selection. *ACS Sustain. Chem. Eng.* **2019**, *7*, 11700–11711. [[CrossRef](#)]
23. Garcia Gonzalez, M.N.; Levi, M.; Turri, S.; Griffini, G. Lignin nanoparticles by ultrasonication and their incorporation in waterborne polymer nanocomposites. *J. Appl. Polym. Sci.* **2017**, *134*, 45318. [[CrossRef](#)]
24. de Carlos Haro, J.; Magagnin, L.; Turri, S.; Griffini, G. Lignin-based anticorrosion coatings for the protection of aluminum surfaces. *ACS Sustain. Chem. Eng.* **2019**, *7*, 6213–6222. [[CrossRef](#)]

25. Lu, J.J.; Cheng, M.Y.; Zhao, C.; Li, B.; Peng, H.H.; Zhang, Y.J.; Shao, Q.J.; Hassan, M. Application of lignin in preparation of slow-release fertilizer: Current status and future perspectives. *Ind. Crop. Prod.* **2022**, *176*, 114267. [[CrossRef](#)]
26. Chen, W.J.; Zhao, C.X.; Li, B.Q.; Yuan, T.Q.; Zhang, Q. Lignin-derived materials and their applications in rechargeable batteries. *Green Chem.* **2022**, *24*, 565–584. [[CrossRef](#)]
27. Budnyak, T.M.; Slabon, A.; Sipponen, M.H. Lignin–inorganic interfaces: Chemistry and applications from adsorbents to catalysts and energy storage materials. *ChemSusChem* **2020**, *13*, 4344–4355. [[CrossRef](#)]
28. de Haro, J.C.; Tatsi, E.; Fagiolari, L.; Bonomo, M.; Barolo, C.; Turri, S.; Bella, F.; Griffini, G. Lignin-based polymer electrolyte membranes for sustainable aqueous dye-sensitized solar cells. *ACS Sustain. Chem. Eng.* **2021**, *9*, 8550–8560. [[CrossRef](#)]
29. Edmeades, R.M.; Hewlett, P.C. Cement admixtures. In *Lea's Chemistry of Cement and Concrete*, 4th ed.; Hewlett, P.C., Ed.; Butterworth-Heinemann: Oxford, UK, 1998; pp. 841–905.
30. Lou, H.M.; Lai, H.R.; Wang, M.X.; Pang, Y.X.; Yang, D.J.; Qiu, X.Q.; Wang, B.; Zhang, H.B. Preparation of lignin-based superplasticizer by graft sulfonation and investigation of the dispersive performance and mechanism in a cementitious system. *Ind. Eng. Chem. Res.* **2013**, *52*, 16101–16109. [[CrossRef](#)]
31. Zheng, T.; Zheng, D.F.; Qiu, X.Q.; Yang, D.J.; Fan, L.; Zheng, J.M. A novel branched claw-shape lignin-based polycarboxylate superplasticizer: Preparation, performance and mechanism. *Cem. Concr. Res.* **2019**, *119*, 89–101. [[CrossRef](#)]
32. Gupta, C.; Nadelman, E.; Washburn, N.R.; Kurtis, K.E. Lignopolymer superplasticizers for low-co<sub>2</sub> cements. *ACS Sustain. Chem. Eng.* **2017**, *5*, 4041–4049. [[CrossRef](#)]
33. Kalliola, A.; Vehmas, T.; Liitia, T.; Tamminen, T. Alkali-O<sub>2</sub> oxidized lignin—A bio-based concrete plasticizer. *Ind. Crop. Prod.* **2015**, *74*, 150–157. [[CrossRef](#)]
34. Li, S.Y.; Li, Z.Q.; Zhang, Y.D.; Liu, C.; Yu, G.; Li, B.; Mu, X.D.; Peng, H. Preparation of concrete water reducer via fractionation and modification of lignin extracted from pine wood by formic acid. *ACS Sustain. Chem. Eng.* **2017**, *5*, 4214–4222. [[CrossRef](#)]
35. Allegretti, C.; Boumezgane, O.; Rossato, L.; Strini, A.; Troquet, J.; Turri, S.; Griffini, G.; D'Arrigo, P. Tuning lignin characteristics by fractionation: A versatile approach based on solvent extraction and membrane-assisted ultrafiltration. *Molecules* **2020**, *25*, 2893. [[CrossRef](#)] [[PubMed](#)]
36. D'Arrigo, P.; Allegretti, C.; Tamborini, S.; Formantici, C.; Galante, Y.; Pollegioni, L.; Mele, A. Single-batch, homogeneous phase depolymerization of cellulose catalyzed by a monocomponent endocellulase in ionic liquid [bmim][cl]. *J. Mol. Catal. B Enzym.* **2014**, *106*, 76–80. [[CrossRef](#)]
37. Allegretti, C.; Fontanay, S.; Rischka, K.; Strini, A.; Troquet, J.; Turri, S.; Griffini, G.; D'Arrigo, P. Two-step fractionation of a model technical lignin by combined organic solvent extraction and membrane ultrafiltration. *ACS Omega* **2019**, *4*, 4615–4626. [[CrossRef](#)]
38. Haist, M.; Link, J.; Nicia, D.; Leinitz, S.; Baumert, C.; von Bronk, T.; Cotardo, D.; Pirharati, M.E.; Fataei, S.; Garrecht, H.; et al. Interlaboratory study on rheological properties of cement pastes and reference substances: Comparability of measurements performed with different rheometers and measurement geometries. *Mater. Struct.* **2020**, *53*, 92. [[CrossRef](#)]
39. Johnson, E.A. Phaffia rhodozyma: Colorful odyssey. *Int. Microbiol.* **2003**, *6*, 169–174. [[CrossRef](#)]
40. Zhang, C.; Chen, X.; Too, H.-P. Microbial astaxanthin biosynthesis: Recent achievements, challenges, and commercialization outlook. *Appl. Microbiol. Biotechnol.* **2020**, *104*, 5725–5737. [[CrossRef](#)]
41. Stachowiak, B.; Szulc, P. Astaxanthin for the food industry. *Molecules* **2021**, *26*, 2666. [[CrossRef](#)]
42. Jacobson, G.K.; Jolly, S.O.; Sedmak, J.J.; Skatrud, T.J.; Wasileski, J.M. Astaxanthin Over-Producing Strains of Phaffia Rhodozyma. U.S. Patent 5,466,599, 14 November 1995.
43. Huang, C.; Chen, X.F.; Xiong, L.; Chen, X.D.; Ma, L.L.; Chen, Y. Single cell oil production from low-cost substrates: The possibility and potential of its industrialization. *Biotechnol. Adv.* **2013**, *31*, 129–139. [[CrossRef](#)]
44. Qadeer, S.; Khalid, A.; Mahmood, S.; Anjum, M.; Ahmad, Z. Utilizing oleaginous bacteria and fungi for cleaner energy production. *J. Clean. Prod.* **2017**, *168*, 917–928. [[CrossRef](#)]
45. EFSA Panel on Nutrition, Novel Foods and Food Allergens (NDA); Allergens, F.; Turck, D.; Castenmiller, J.; de Henauw, S.; Hirsch-Ernst, K.-I.; Kearney, J.; Maciuk, A.; Mangelsdorf, I.; McArdle, H.J.; et al. Safety of *Yarrowia lipolytica* yeast biomass as a novel food pursuant to regulation (eu) 2015/2283. *EFSA J.* **2019**, *17*, e05594.
46. Wei, Y.; Siewers, V.; Nielsen, J. Cocoa butter-like lipid production ability of non-oleaginous and oleaginous yeasts under nitrogen-limited culture conditions. *Appl. Microbiol. Biotechnol.* **2017**, *101*, 3577–3585. [[CrossRef](#)] [[PubMed](#)]
47. Cho, H.U.; Park, J.M. Biodiesel production by various oleaginous microorganisms from organic wastes. *Bioresour. Technol.* **2018**, *256*, 502–508. [[CrossRef](#)]
48. Yi, J.S.; Yoo, H.W.; Kim, E.J.; Yang, Y.H.; Kim, B.G. Engineering streptomyces coelicolor for production of monomethyl branched chain fatty acids. *J. Biotechnol.* **2020**, *307*, 69–76. [[CrossRef](#)]
49. Ran-Ressler, R.R.; Khaïlova, L.; Arganbright, K.M.; Adkins-Rieck, C.K.; Jouni, Z.E.; Koren, O.; Ley, R.E.; Brenna, J.T.; Dvorak, B. Branched chain fatty acids reduce the incidence of necrotizing enterocolitis and alter gastrointestinal microbial ecology in a neonatal rat model. *PLoS ONE* **2011**, *6*, e29032. [[CrossRef](#)]
50. Wang, X.; Xiaohan, W.; Chen, Y.; Jin, W.; Jin, Q.; Wang, X. Enrichment of branched chain fatty acids from lanolin via urea complexation for infant formula use. *LWT Food Sci. Technol.* **2020**, *117*, 108627. [[CrossRef](#)]
51. Wang, W.; Lee, D.-J. Lignocellulosic biomass pretreatment by deep eutectic solvents on lignin extraction and saccharification enhancement: A review. *Bioresour. Technol.* **2021**, *339*, 125587. [[CrossRef](#)]

52. Procentese, A.; Raganati, F.; Olivieri, G.; Russo, M.E.; Rehmann, L.; Marzocchella, A. Deep eutectic solvents pretreatment of agro-industrial food waste. *Biotechnol. Biofuels* **2018**, *11*, 37. [[CrossRef](#)]
53. Taherzadeh, M.J.; Karimi, K. Pretreatment of lignocellulosic wastes to improve ethanol and biogas production: A review. *Int. J. Mol. Sci.* **2008**, *9*, 1621–1651. [[CrossRef](#)]
54. Sar, T.; Arifa, V.H.; Hilmy, M.R.; Ferreira, J.A.; Wikandari, R.; Millati, R.; Taherzadeh, M.J. Organosolv pretreatment of oat husk using oxalic acid as an alternative organic acid and its potential applications in biorefinery. *Biomass Conv. Bioref.* **2022**. [[CrossRef](#)]
55. Allegretti, C.; Fontanay, S.; Krauke, Y.; Luebbert, M.; Strini, A.; Troquet, J.; Turri, S.; Griffini, G.; D'Arrigo, P. Fractionation of soda pulp lignin in aqueous solvent through membrane-assisted ultrafiltration. *ACS Sustain. Chem. Eng.* **2018**, *6*, 9056–9064. [[CrossRef](#)]
56. Faix, O. Fourier transform infrared spectroscopy. In *Methods in Lignin Chemistry*; Lin, S.Y., Dence, C.W., Eds.; Springer: Berlin/Heidelberg, Germany, 1992; pp. 83–109.
57. Boeriu, C.; Bravo, D.; Gosselink, R.; Dam, J. Characterisation of structure-dependent functional properties of lignin with infrared spectroscopy. *Ind. Crop. Prod.* **2004**, *20*, 205–218. [[CrossRef](#)]
58. Rencoret, J.; Prinsen, P.; Gutiérrez, A.; Martínez, Á.T.; del Río, J.C. Isolation and structural characterization of the milled wood lignin, dioxane lignin, and cellulolytic lignin preparations from brewer's spent grain. *J. Agric. Food Chem.* **2015**, *63*, 603–613. [[CrossRef](#)] [[PubMed](#)]
59. He, W.M.; Fatehi, P. Preparation of sulfomethylated softwood kraft lignin as a dispersant for cement admixture. *RSC Adv.* **2015**, *5*, 47031–47039. [[CrossRef](#)]
60. Takahashi, S.; Hosoya, S.; Hattori, M.; Morimoto, M.; Uraki, Y.; Yamada, T. Performance of softwood soda-anthraquinone lignin-polyethylene glycol derivatives as water-reducing admixture for concrete. *J. Wood Chem. Technol.* **2015**, *35*, 348–354. [[CrossRef](#)]
61. Childs, C.M.; Perkins, K.M.; Menon, A.; Washburn, N.R. Interplay of anionic functionality in polymer-grafted lignin superplasticizers for portland cement. *Ind. Eng. Chem. Res.* **2019**, *58*, 19760–19766. [[CrossRef](#)]
62. Ji, D.; Luo, Z.Y.; He, M.; Shi, Y.J.; Gu, X.L. Effect of both grafting and blending modifications on the performance of lignosulphonate-modified sulphonic acid-phenol-formaldehyde condensates. *Cem. Concr. Res.* **2012**, *42*, 1199–1206. [[CrossRef](#)]